CARBONIZING COMPRESSED HYDROXYETHYL CELLULOSE UTILIZING STRESS RELAXATION – AN EFFECTIVE WAY TO TUNE PORE STRUCTURE OF ACTIVATED CARBON

CHEN FUXIANG

(B. Eng. (Hons.), NUS

A THESIS SUBMITTED

FOR THE DEGREE OF MASTER OF ENGINEERING

DEPARTMENT OF CHEMICAL AND BIOMOLECULAR ENGINEERING

NATIONAL UNIVERSITY OF SINGAPORE

2012

Acknowledgements

I would first like to express deep appreciation for the financial support by the NRF/ CRP "Molecular engineering of membrane research and technology for energy development: hydrogen, natural gas and syngas" (R-279-000-261-281).

I would also like to thank A/P Hong Liang for his kind guidance in the course of 2 years and my colleagues for providing me assistance in the laboratories. Equally important, I would like to express my gratitude for NUS for providing the opportunity for me to further my education as well as a chance to fulfill a milestone in my life.

Last, but not the least, my family and friends, especially a friend with a special place in my heart, for their unquestioned supports over these years.

Summary

Activated carbons (AC) are widely studied as an adsorbent and a variety of preparation methods have been widely established. Sophisticated synthesis methods or using chemical agents that have detrimental environmental impacts are usually utilized to produce highly porous carbons. In this work, the feasibility of implementing a simple pre-treatment process prior carbonization to enhance pore formation of AC is explored. AC are synthesized using hydroxyethyl cellulose (HEC) powder as the precursor. Commercial HEC powder is compressed at different conditions (e.g. compressive force and holding time) to induce deformation of HEC-chain conformations from their initial states. The different stress exerted on the pellets due to the effects of different compression conditions affect the degree of "quasi" crosslink networks formed. Pyrolyzing polymer chains at elevated stress states influences the formation of the carbonaceous backbones and the moieties. The slow stress relaxation due to the "quasi" crosslink networks between side-chain groups is postulated to be the key factor in contributing to formation of porous carbons.

N_2 adsorption tests suggest cold compression of HEC prior carbonization is effective in producing highly porous carbon powder. Microscopic analysis by FESEM reveals different structural traits can be derived under different synthesis conditions. Studies on the carbon backbones by ^{13}C NMR and chemical functionalities by FTIR and XPS suggest variations of surface oxygen functionalities produced due to effects of the pre-treatment are postulated to have structural impacts on the carbon structure. Inadvertently, the basicity of the AC produced is also affected. Hydrogen sulfide adsorptions assessments show the effect on surface-area expansion and basicity of the AC produced by this physical treatment approach.

Table of Contents

List of Figures

List of Tables

List of Illustrations

1 Introduction

Porous or activated carbon (AC) is conventionally used as an absorbent for water and gas purification applications. It is an irreplaceable material due to the high adsorption capability and the cost effectiveness of the production. These advantages, along with the increasing challenges in technological aspects, provide motivations for the exploration of applications of carbon in other frontiers. Porous carbon has found to be an effective adsorbent for bio-molecules [1, 2], a material for the synthesis of electrode of super capacitor [3] and an effective storage medium for natural gas [4-6]. The rapid development in the diverse applications of porous carbon is an indication of its importance in material science. Factors influencing the development of the pore characteristics (e.g. porosity, pore size distribution, and types of pores) of porous carbon materials have been well established in pioneer works. Some of the factors are "(a) parent feedstock (b) heating rate (c) flow of containing gas (d) final heat treatment temperature (HTT) of carbonization (e) the temperature of activation (f) the activating gas (g) the duration of activation (h) flow rate of the activating gas (i) the experimental equipment used [7]". Synthesis of porous carbons revolves around the manipulation of these factors. Creative solutions such as surface modifications and nano-casting can further improve the pore characteristics of carbon. These solutions enhances the properties of the AC by improving the surface functionalities [8-10] and controlling the pore size and the pore size distributions [3]. The drawbacks for these solutions are the high complexity and the cost associated with the synthesis process. In addition, chemicals that are considered to have detrimental effects on the environment may be utilized to facilitate the development of porous structures in the AC. The range of pros and cons related to various synthesis techniques suggest rooms for further development on the synthesis techniques of porous carbons.

Porous carbons can be produced in the powdered form or a more defined bodily form such as carbon monoliths. Carbon monoliths demonstrate higher mechanical strength and stability compared to AC powder and is used in applications involving pressurized environment

applications such as storage of natural gas [4, 6, 11, 12]. Traditionally, a compressive force (CF) is employed to increase the bulk density and the mechanical stability of the carbon monoliths. Since the CF essentially creates a densification effect, some degree of loss of porosity is to be expected [13] and additional processing are required to redevelop the lost porosity.

The feasibility of using CF as a means to produce highly porous carbon is hard to fathom and could be the root cause for the lack of literature works based on this hypothesis. Since the structural response of the material towards CF is dependent on its intrinsic properties [13], research potentials pertaining to developing porous structure using CF exist. In particular, in polymeric bodies, the equilibrium between polymer chain deformation or changes in free volume and the stress applied is hard to fathom due to the dynamic nature of visco-elastic properties. The kinetics of chain motion to resume equilibrium state after the removal of the load is affected by the chain structures (flexibility and type of side-chain groups) and the chain packing density. Thus, the stress relaxation behavior upon removal of the applied stress of polymeric bodies is not discrete. Scission of polymer chains promotes rapid stress relaxation [14] and simultaneously, the formation of the polyaromatic hydrocarbon (PAH) structures by aromatization. The pyrolysis of the polymeric material before it resumes the equilibrium state would therefore produce a variety of carbon structures. The kinetics associated with stress relaxation during carbonization invariantly influences the development of the pore characteristics of the carbon formed.

This thesis investigates the effect of cold compression of a cellulose based polymer prior pyrolysis. This methodology is favored due to the simplicity and cost effectiveness of the implementation compared with other pore-forming methods. In this study, porous carbons are synthesized using 2-hydroxyethyl cellulose (HEC) as the precursor. The pendant hydroxyl ethyl side-chain group of HEC has been established to be effective in producing highly porous AC matrices [15]. The changes to the pore texture, turbostraticity (stacking flaws) of PAHs, and the chemical functionalities of the carbon bodies will be scrutinized to develop insights on the

hypothesis. The practicability of the porous carbons synthesized is determined by the adsorption capability for H_2S gas. Since H_2S is a highly toxic pollutant that is present in high concentration in natural gas, a distinct improvement in the adsorption performance will provide validation for the effectiveness of the feasibility of the pre-treatment.

2 Literature Review

The objective of this section is to provide a brief overview and some background information that has relevance to this work.

2.1 Surface oxygen complexes on carbon surfaces

Although carbonization removes most of the heteroatoms present in the material, formation of surface oxygenated complexes are inevitable. The presence of the surface oxygen complexes can affect chemical reactivity during thermal activation as well as influencing the surface basicity of the carbon species.

2.1.1 Thermal activation

Highly porous carbon materials are usually not attainable by solely carbonizing the precursors. An activation process usually accompanies the carbonization process to further improve the porosity of the carbon material formed. Activation processes are categorized into 2 classifications: thermal and chemical activation. Thermal activation, otherwise also known as physical activation, involves the use of an oxidizing gas, namely carbon dioxide, steam and in rare occurrence, oxygen. Based on the following stoichiometric equations, the porosity of the carbon material is improved by 'removing' carbon atoms from the surface of the carbon material:

$$C + CO_2 \rightarrow 2\,CO$$

$$C + H_2O \rightarrow CO + H_2$$

The actual mechanisms involved in the thermal activation process are complex and generalizing the mechanisms is near impossible. This is because the reaction mechanisms are temperature dependent. Primarily, the mechanisms involve understanding the role of the production of the chemisorbed oxygen complexes formed [7]. During the activation process, the surface oxygen complexes can serve dual functions. The formation of wide range of surface oxygen complexes

generates a reservoir of reaction intermediates with a wide range of functionalities and chemical stabilities. Hence, a large range of possible reaction mechanisms can occurs. However, the more chemically stable surface oxygenated complexes can also compete for reaction sites, retarding the rate of gasification. The development of porous structure can be influenced by the presence of the surface oxygenated complexes.

2.1.2 Surface acidity and basicity

AC can exhibit surface acidity and basicity when placed in pure water and equilibrium is allowed to be established [16]. It may be straightforward to infer that the acidity of the water is due to the dissociation of a proton from a surface oxygenated group present in the AC, the contribution towards the surface basicity of carbon surface remains unclear. Two schools of thoughts developed from pioneer works suggest that the delocalized π-electrons of graphene layers and the surface oxygenated complexes present in the AC are key factors contributing to the surface basicity. Firstly, the delocalization of the π-electrons in graphene layers promotes basicity behavior through the adsorption of protons from water solution by the following equation:

$$C_\pi + H_3O^+ \rightarrow C_\pi - H_3O^+$$

Leon *et al* (1992) [7] established that the formation of this electron donor addition complex is predominant in carbons with low oxygen contents. Since each H_3O^+ ion is associated with the graphitized carbon, the basicity is hence also dependent on the accessibility of the ions to the available sites.

From the perspective from molecular orbital calculations, the regions near the edges of graphene have a strong influence in the distribution of the π-electrons. Typically, 2 forms of shapes exist, and the zigzag configuration is chemically more reactive and conductive than the armchair configuration. Thus, the edges with zigzag configuration exhibit localizations of electrons while the arm chair allows a more uniform distribution of the electron density. Upon thermal activation,

gasification reduces the size of the graphene layers, thereby promoting localization of the π-electrons. In addition, the localization can further be enhanced by the presence of the acidic oxygenated groups produced by gasification. As a result of the localization, the surface basicity of the carbon planes decreases. Consequently, the adsorption capability of the AC formed may be affected by the reduction in basicity.

2.2 Synthesis of Porous Carbons

2.2.1 Chemical Activation and Surface Modification

Carbon surfaces are modified to enhance the adsorption capability of a specific species. Thermal activation, discussed in Section 2.1.1, modifies the carbon surfaces by generating surface oxygenated complexes. However, a larger extent of surface modification is achievable by chemical activation. A chemical agent such as a dehydrating agent ($ZnCl_2$ or H_3PO_4) or a strong base or acid [9] can be employed in developing a range of porosity, surface morphologies [17] and surface complexes. Chemical agents can also be used to introduce specific functionalities to enhanced adsorption performance. For instance, ammonia has been used to [18] incorporate nitrogen functionality on carbon surfaces and has been proven to be effective in enhancing adsorption of sulphur content due to the increased surface basicity [18, 19]. However, ammonia is a hazardous chemical that pose negative impacts to the environment. In addition, chemical agents that are non-degradable by thermal treatment reside within the carbon structure at the end of the manufacturing process. Thorough post-treatments are necessary and chemical wastes are generated. Using chemical agents to produce porous carbons is deemed to be less environmental friendly and more process intensive.

2.2.2 Nano-casting

Porous carbons developed from nano-casting are used in high performance electrode materials applications due to the high surface area and narrow pore size distribution of the carbon material.

Nano-casting can be classified into hard templates or soft templates techniques. Porous carbons are synthesized by impregnating the precursors within with porous silica template hard templates or mixed with organic molecules. Polymerization of the precursors develops the organo matrix in the templates. Subsequently, carbonization converts the organo matrix into an ordered carbon structure. In hard template techniques, the silica structure has to be removed by HF to create an ordered porous carbon structure. In soft template techniques, carbonization removes the soft carbon and a porous hard carbon matrix is developed. In most synthesis processes, a high content of mesopores are developed from soft templates. Activation may be utilized to redevelop micropores in the porous structure.

Hard template techniques are generally less preferred compared to soft template techniques due to the use of high toxicity and corrosive properties of HF in the post-treatment. In both techniques, addition of a suitable catalyst is often necessary to facilitate the development of the organo-matrix and a considerable amount of time is necessary to develop the polymer matrix. Development of porous carbon from templates may produce high surface area with narrow pore size distribution may be possible and in exchange, the manufacturing process is deemed to be tedious and costly.

2.3 Effect of compressive forces on porous materials

J. Alcañiz-Monge *et al* and co-workers [13] investigate the effect of compression on different materials and concluded that compressive forces on the bodies reduces the pore volume and interstitial void spaces. What is of higher relevance is the establishment that “porous solids with organic framework and a low mechanical resistance are largely affected by compression”. J. Alcañiz-Monge *et al* further established that with increasing compressive force, a change in the pore texture of the porous organic framework is observed. A sequential development: the disappearance of the mesopores, followed by the micropores and eventually the narrow micropores changes of the pore texture of the porous organic matrix with increasing compression force.

The reduction in porosity in porous organic structure due to effects of compression may not be desired in the synthesis of AC produced from thermal activation. This is because thermal activation is a diffusion dependent process and a longer activation period is necessary to redevelop the porosity of the carbon structure [6]. The changes in the pore size distribution due to effects of compression influence applicability and the efficiency of the carbon materials.

2.4 Stress energy and cross-links

From the statistical theory of rubber elasticity, it can be inferred that the elastic stress of a linear elastomer under axial extension is directly proportional to the concentration of network chains formed [20]. Under the influence of stress, the re-orientation and creeping of the polymer chains inevitably cause deformation. To attain a equilibrate state of stress within the matrix, chain motions have to be curbed and locked by some mechanism. This is achieved by developing networks of cross linkages in the polymer matrix. Without the cross-links, the polymer chains slide over each other and are unable to exhibit stress. The cross-linkages can be achieved by chemical means but what is worth more of an attention is the effect of "quasi-crosslink". "Quasi-crosslink" arises due to the entanglement of the chains. Under the influence of stress, the polymer chains are of a closer proximity with each other. Hence, the amount of the entanglement developed is also considerable. As the formation of these "quasi-crosslink" poses additional conformation restrictions, the amount of elastic stress arising from the large amount of "quasi-crosslink" is significant.

2.5 Stress Relaxation

Upon the removal of the stress, the polymeric materials are likely to subject to exhibit relaxation behaviors in 2 main ways: physical means by gradual motion of the polymer chains to undo the entanglement and by chemical means. The chemical relaxation process is the relaxation rising from chemical changes and has a higher implication issues in processing applications. Due to

changes in the chemical structures of the polymer chains, chemical relaxation is predominant at high temperature operations [14].

3 Experimental Materials and Methods

3.1 Preparation of polymer pellets

2-hydroxyethyl cellulose powder (HEC) (Sigma Aldrich, average molecular weight of 250,000) is used directly from the packaging without prior treatment. A 3.125 cm diameter pellet die set is filled with known masses of HEC powder and CF is exerted gradually on the HEC powder using a manual hydraulic press (maximum load of 10 metric ton) to synthesize the polymer pellets (Figure 3.1). The CF is maintained at a stipulated duration of 15 or 60 minutes. At the end of the holding duration, the load on the pellet is slowly removed and the pellet extracted out from the die set.

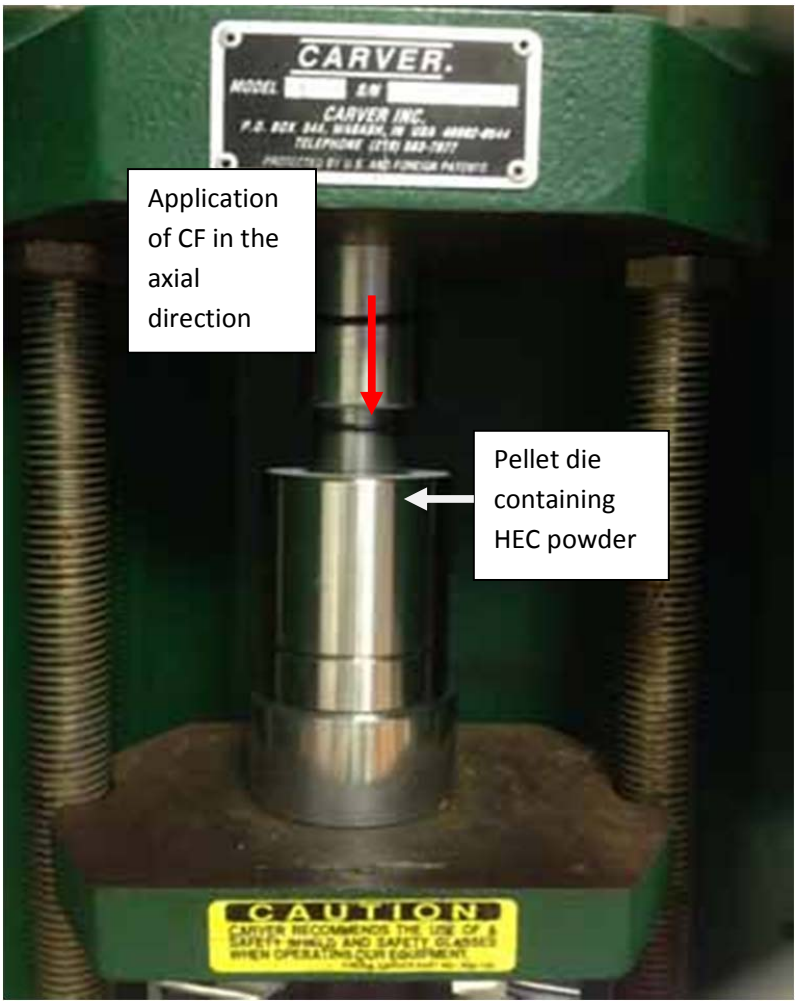

Figure 3.1: Synthesis of HEC pellets using a manual hydraulic press

3.2 Synthesis of AC

The conditions of synthesis of AC from HEC has been studied in previous work by Sun *et al* [15] and the conditions are adopted. The high thermal treatment reactions (HTT), are carried out in a tubular quartz reactor tube (diameter: 50mm; length 1200 mm). The polymer pellets are placed on a ceramic plate positioned in the middle of the reactor. The reactor is enclosed with the use of stainless steel clamps, O-rings and securing screws (Figure 3.2). The carbonization process is carried out at 400°C for 1 hour in an argon environment. Subsequently, the carbonaceous material produced is activated at 700°C for 2 hours in carbon dioxide environment. The AC is allowed to cool down to room temperature. The ramp rate used for both carbonization and activation processes is 5 °C/min and the flow rate of both the argon and the carbon dioxide used is 500 cm^3/min. The AC pellets are crushed into fine powder using a mortar and a pestle. The AC are washed several times with distilled water before dried in an oven.

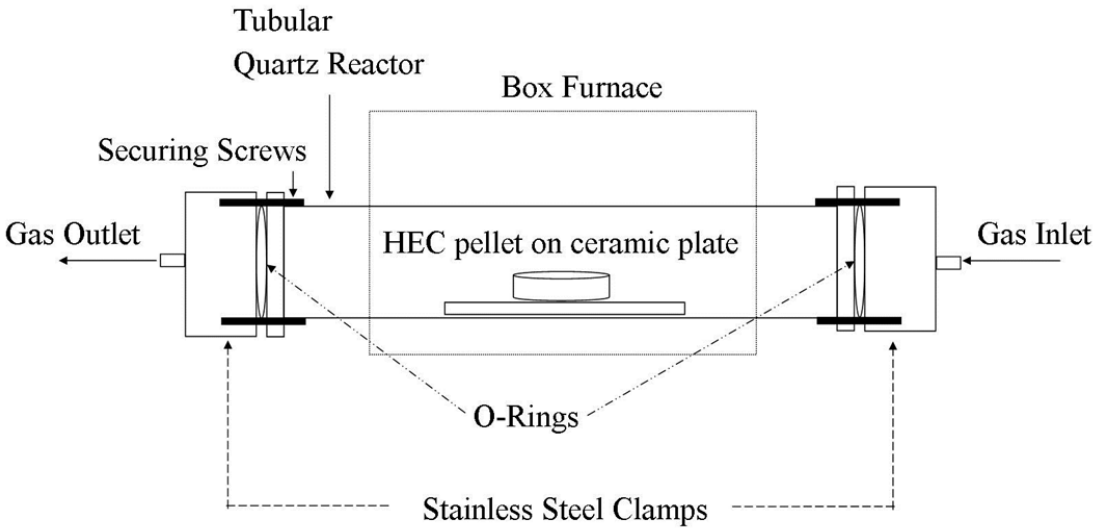

Figure 3.2: Experimental set up for the HTT reactions

3.3 Sample naming and notations

Samples are named in the format of X-X-X-Y. The first prefix denotes the mass loading of HEC, the second prefix represents the CF which the HEC powder is subjected to and the third prefix

represents the holding duration of the CF. A suffix “AC” refers to the AC’ formed after activation in carbon dioxide environment at 700°C. A suffix “C” refers the carbonaceous materials formed after pyrolysis at 400°C. A suffix “P” refers to HEC pellets synthesized prior the carbonization process.

In this work, the term “carbonaceous material” is used frequently and it should be highlighted that this term refers to the carbon material produced after carbonization at 400ºC.

3.4 Characterization

3.4.1 Surface area and pore size analysis by N_2 adsorption

The pore characteristics of the AC are analyzed using a Quantachrome Autosorb-1 Series surface area and pore size analyzer. The AC samples are first degassed in vacuum at 300°C for 3 hours. Nitrogen gas is used as the adsorbent gas and the characterization is carried out at 77K using liquid nitrogen. The surface area of the AC, S_{BET} is determined by using the Brunauer-Emmett-Teller (BET) model at relative pressure P/P_0 in the range of 0.05 to 0.30. The total pore volume (V_t) is determined using the Barret-Joyner-Halenda (BJH) model with reference to the relative pressure P/P_0 at 0.99. In addition, the micropore volume (V_{micro}) was determined by Dubinin-Redushkevich (DR) method. In this study, the mesopore volume (V_{meso}) is estimated by taking the difference between V_t and V_{meso}. The non-linear density functional theory (NLDFT) is used to determine the pore size distribution of the AC.

3.4.2 Surface morphology: FESEM

The structural morphologies of the AC are examined using a field-emission scanning electron microscope (FESEM, JEOK, JSM-6700F, Japan). The carbon samples are coated with platinum for duration of 90 seconds at a current of 30 mA prior each analysis.

3.4.3 Functional groups characterization

The surface functionalities of the carbonaceous materials are determined by X-ray photoelectron spectroscopy (XPS, Kratos Axis His System). The binding energy of C 1s of 284.6 eV is used as the reference for other functionalities in the peak fitting process. Peaks are fitted using Gaussian model with a Shirely baseline [15, 21]. The solid-state CP/MAS of the ^{13}C spectra of the carbonaceous materials are obtained using Bruker Avance 400 (DRX400). The samples are also characterized by Fourier transform infrared spectroscopy (FTIR). Prior each analysis, minute quantities of the carbon samples are mixed with KBR powder. The mixtures are compressed for duration of 30 seconds at 6 metric ton to form the analysis pellet.

3.4.4 Surface Basicity

0.1 g of the AC samples is dispersed in 80ml of distilled water. The mixture is left overnight to allow equilibrium to be established. The pH of the water is measured using Fisher Accumet Basic AB15 pH Meter at ambient temperature and is used as an indication of the surface basicity of the AC samples.

3.4.5 H_2S Adsorption Test

The H_2S adsorption capability of the AC is conducted at ambient temperature in a quartz tubular fixed bed reactor (diameter of 10mm, length of 200mm). In each run, 0.13 g of the carbon absorbent is packed by tapping gently with a metal rod. A mixture of H_2S (1000 ppm) and nitrogen gas is fed into the bed column at a flow rate of 1000 cm^3/hr. The concentration of H_2S in from the outlet of the reactor is monitored over time and measured using an electro-chemical sensor (MOT500-H2S, Keernuo Electronics Technology). The flow is maintained until the bed is fully saturated. The breakthrough concentration is defined at 10ppm (equivalent to C/C_0 value of 1%) and the breakthrough time as the total time taken to detect this amount of H_2S. The breakthrough capacity of H_2S is then calculated based on the following equation [22]:

$$Breakthrough\ capacity\ \left(\frac{mg\ H_2S}{g\ Carbon}\right) = \frac{Q\left(\frac{ml}{min}\right) x\ t\ (\text{min})\ x\ C_{H_2S}(ppm)\ x\ M_{H_2S}(\frac{g}{mol})}{22.4(\frac{l}{mol})x\ m_{carbon}(g)x\ 10^6}$$

where Q is the flow rate of the feed gas, t is the breakthrough time, C_{H_2S} is the inlet concentration of H_2S, M_{H_2S} is the molecular weight of H_2S, and m_{carbon} is the mass of the carbon sample used.

4 Results and discussion

4.1 Impact of cold compression on pore characteristics of AC

4.1.1 Preliminary study on the effect of cold compression

The effectiveness of implementing cold compression prior the HTT processes is first determined by comparing the pore characteristics of AC produced from a fixed quantity of 5 g of HEC under different compression conditions. The pore characteristics of the AC are characterized using N_2 adsorption and the findings are reported in Figure 4.1. In Figure 4.1, experimental data correspond to a zero CF represents the pore characteristics of AC produced without cold compression. The preliminary findings report that the absence of cold compression pretreatment results in the synthesis of AC with the lowest S_{BET} and pore volume. Evidently, the implementation of cold compression prior carbonization improves the quality of the AC synthesized.

4.1.2 Influence of CF and holding duration on pore characteristics of AC

It is also reported in Figure 4.1 that the effectiveness of the methodology is dependent on both compression parameters (CF and holding time). The findings first show that the increase in the CF has the inclination to improve the pore characteristics of the AC synthesized using the proposed methodology. However, the influence of the CF on the resulted pore characteristics of the AC is also dependent on the holding duration of the applied force. For instance, for a holding duration of 15 minutes, an incremental improvement in the pore characteristics of the AC produced is reported when the CF increases from 2 to 4 metric ton. However, further increase in the CF does not generate considerable improvement in the pore characteristics of the AC. On the contrary, for a holding duration of 60 minutes, the incremental improvement in the pore characteristics of the AC produced can be observed over the range of the CF used. It is also noted that AC of similar pore characteristics synthesized using a holding duration of 15 minutes can be replicated using a holding duration of 60 minutes but at a lower CF. For example, it is reported that the sample 5-4-

15-AC has an average S_{BET} of 1400 m^2/g and pore volume of 0.83 cc/g. If a holding duration of 60 minutes were to be used, the AC with similar characteristics may be produced at a CF of 2 metric ton instead of 4 metric ton. It is evident that the synthesis of AC from a mass loading of 5 g of HEC is more effective when a longer holding duration is used in the cold compression step. In particular, the combination of high CF and longer holding duration would yield AC with the most optimal pore characteristics.

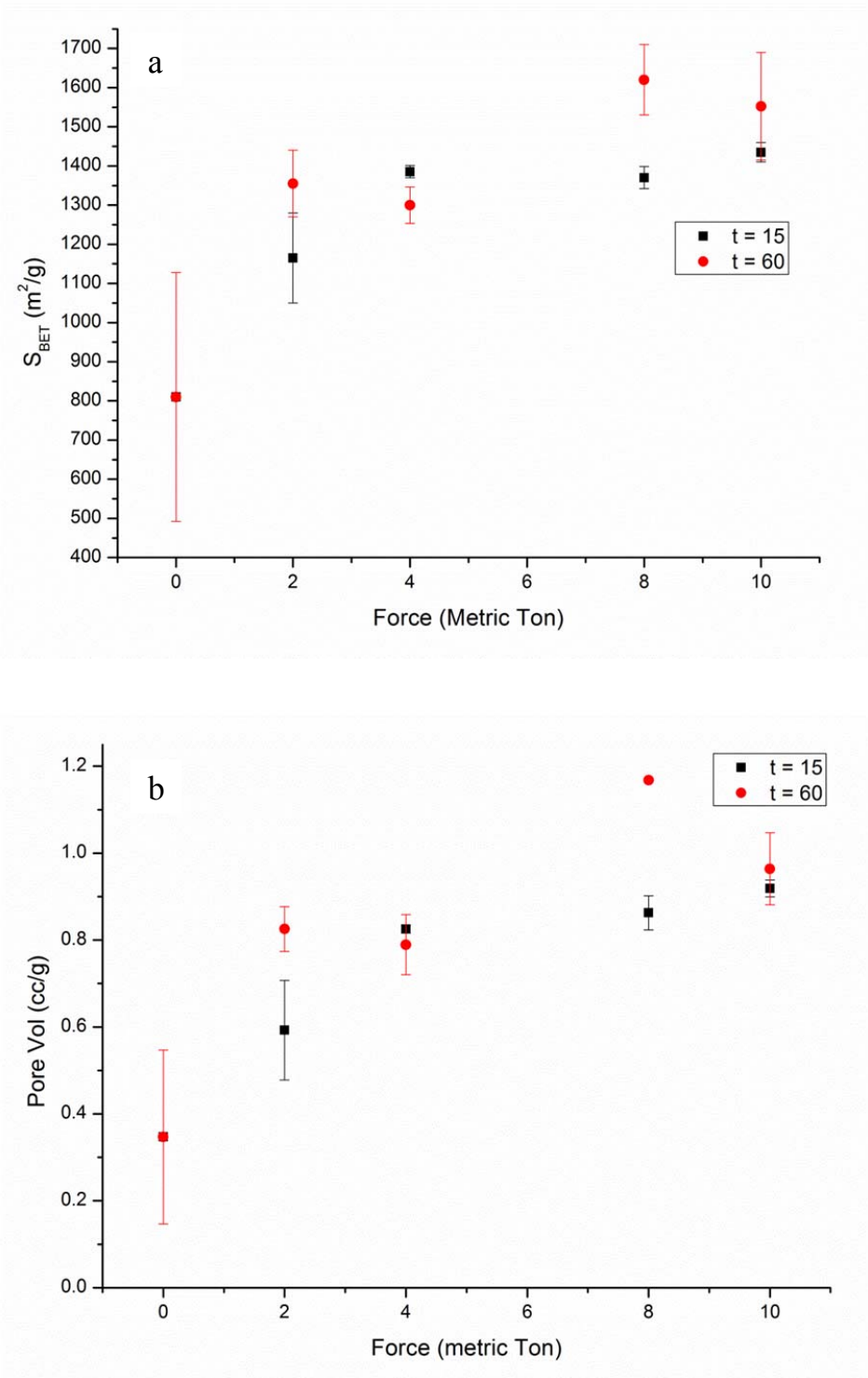

Figure 4.1: Pore characteristics (S_{BET} (a) and pore volume (b)) of the AC synthesized from 5 g of HEC pellets. AC synthesized

4.1.3 Impact of thickness of pellet on the pore characteristics of AC

Table 4.1: List of physical attributes of HEC pellets after cold compression and the corresponding pore characteristics of AC synthesized

Pellets				AC	
Sample	Thickness, x (cm)	Δx (cm)	Bulk Density, (kg/m^3)	S_{BET} (m^2/g)	Pore Volume (cc/g)
5-2-15-P	5.69	(reference)	115	1170	0.59
5-2-60-P	5.55	0.14	117	1360	0.83
5-8-15-P	5.25	0.44	124	1370	0.86
5-8-60-P	5.14	0.55	127	1620	1.17
2.5-2-15-P	2.79	(reference)	117	1580	1.07
2.5-2-60-P	2.67	0.12	122	1080	0.62
2.5-8-15-P	2.65	0.14	122	2080	1.43
2.5-8-60-P	2.56	0.23	127	1790	1.30
3.75-8-15-P	3.97	-	123	1740	1.05

A comparative study on the effect of the thickness of the pellets synthesized on the pore characteristics of the AC has also been included in this work. The thicknesses of the pellets are determined by the mass loading of HEC powder used (2.5g and 5g). In this work, HEC pellets synthesized from a mass loading of 2.5 g correspond to a 'thin' pellet and pellets synthesized from a mass loading of 5 g will correspond to a 'thick' pellet. However, the mass loading is used as the investigation parameter for experimental convenience. The physical characteristics of the pellets after effects of CF and the key findings of the pore characteristics of the AC synthesized are tabulated in Table 4.1.

The effect of cold compression on the pore characteristics of AC is dissimilar when HEC pellets of different thickness are used. Although the increase in CF to improve the pore characteristics of the AC is unbiased to the thickness of the pellet synthesized, the effectiveness is amplified when a thin pellet is used. Under the same compression conditions (CF and holding duration), AC of a higher S_{BET} and pore volume can be synthesized using a thin pellet. For example, while the sample 5-8-15-AC yield a S_{BET} and pore volume of 1370 m^2/g and 0.86 cc/g respectively, it is reported that 2.5-8-15-AC has a much larger S_{BET} and pore volume of 2080 m^2/g and 1.43 cc/g respectively (Table 4.1). Essentially, the findings report that using a thin HEC pellet is highly advantageous to synthesize porous AC: firstly, a more optimal use of the quantity of the precursors reduces the material cost of the synthesis process. Secondly, additional cost savings can arise from the usage of a lower amount of compression energy (due to a lower CF used) and at a faster rate of synthesis (due to a shorter holding duration).

One may claim that the change in the quantity of the precursors used may have a major influence over the properties of the AC synthesized. The effect of the mass loading on pore formation can be investigated further in the following study: Different quantity of HEC powder (2.5 g, 3.75 g and 5 g) are used to synthesize HEC pellets at a compression condition of 8 metric ton for 15 minutes. The corresponding thicknesses of the pellets synthesized are 2.65 cm, 3.97cm and 5.25 cm respectively and are tabulated in Table 4.1. The pore characteristics AC derived from these pellets are compared with AC derived using the same set of mass loading but without cold compression (Figure 4.2). Firstly, it is reported that in the absence of cold compression, the changes in the mass loading of the HEC powder used in the synthesis of AC have negligible impact on the pore characteristics of the AC. Conversely, a substantial increase in the average S_{BET} from 1370 m^2/g to 2075 m^2/g and the average pore volume of 0.85 cc/g to 1.46 cc/g is achieved by decreasing the mass loading of the pellets used. Essentially, the results demonstrate that the quantity of the precursors used does not have a prominent impact on the pore formation of AC. In addition, from

Table 4.1 a similar conclusion can be obtained based on other compression conditions. It is evident that although the mass loading inherently determines the thickness of the pellets synthesized under a set of compression conditions, the thickness of the HEC pellets is the primary attribute that influences the quality of the AC produced.

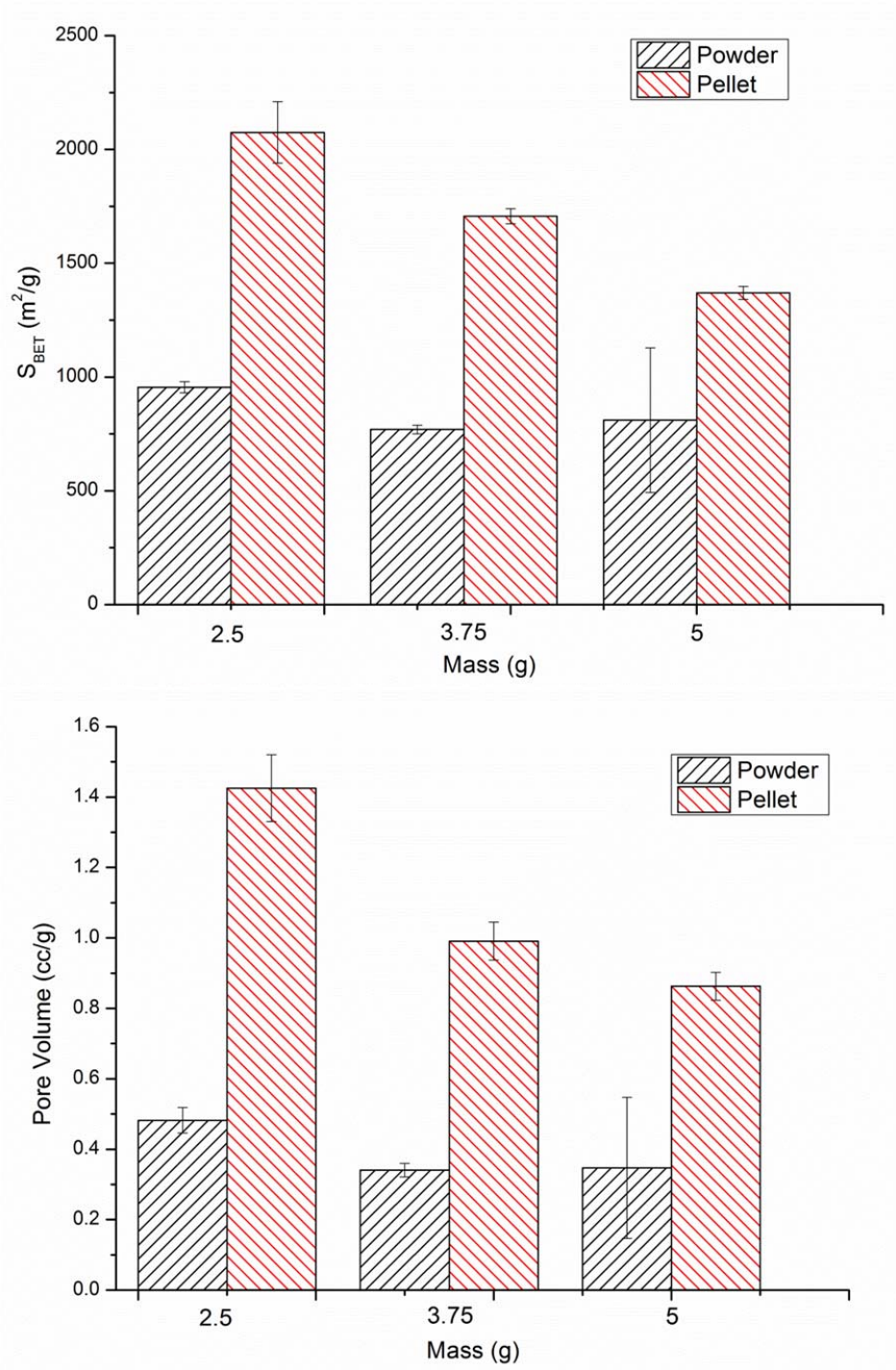

Figure 4.2: Comparative study on effect of variation of mass loading on the S_{BET} (a) and pore volume (b) of the AC produced with and without cold compression pre-treatment

It is reported in Section 4.1.2 that the combination of high CF and longer holding duration favors the formation of AC with better pore characteristics using thick (5 g) HEC pellets. However, from the results in Table 4.1, the findings show that the combination of high CF with longer holding time has a negative impact on the quality of the AC produced from thin pellets. It is evident that the thicknesses of the pellets also influence the effect of the holding duration on the pore characteristics of the AC. Further discussion on the ambiguity will be provided in Section 4.3.2.

4.2 Formation of "quasi" crosslinks networks by cold compression driven chain motion

The phenomenon observed is closely related to the effect of creep (chain motion) and the development of the "quasi" crosslink networks due to the effect of cold compression. In the absence of CF, each HEC polymer chain exists in its own initial stress equilibrium. The equilibrium is maintained by development of intra-chain physical cross linkages by the pendant groups with the main backbone chain (Illustration 4.1). Several polymer chains may form inter-chain "quasi" crosslinks with each other and adopt the shape of a spherical powder granule. Under the influence of external stress, polymer chains exhibit creep. Portions of the chains from 1 powder granule can slide into neighboring powder granules, forming a larger extent of physical inter-chain cross linkages with each other. The formation of the inter-chain "quasi" crosslink networks reduces the free volume in the spherical granules and enhances the mechanical support of the entire matrix (Illustration 4.1).

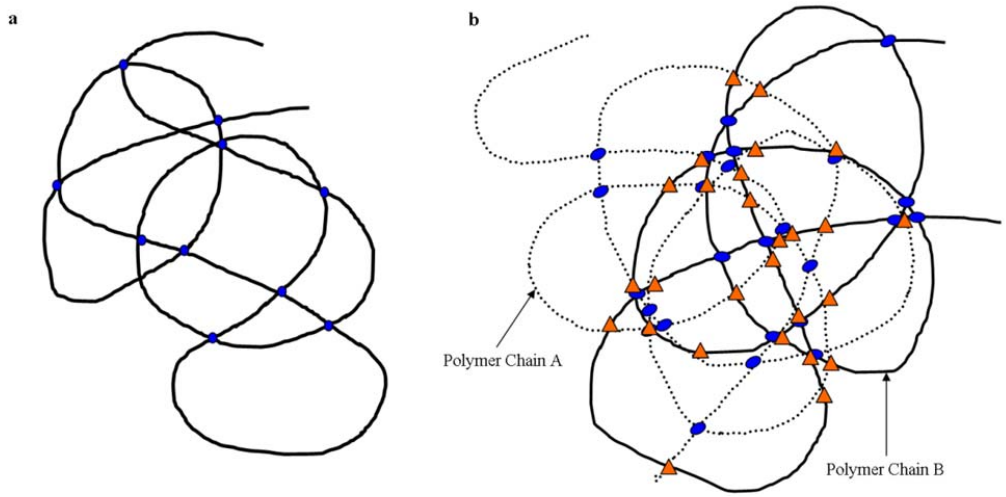

Illustration 4.1: Schematics representing different states of the polymer chains: a) represents a single HEC polymer chain and b) 2 polymer chains under effect of creeping by compression. Circles represent intra-chain "quasi" cross linkages and triangles represent inter-chain "quasi" cross linkages

The increased number of “quasi” crosslink networks formed establishes new stress equilibrium in the polymer pellets as described in Section 2.4. The compressive stress energy stored within the network may be utilized during the HTT processes for development of structural features. It is apparent that the increase in the CF results in a larger amount of stress energy stored within the polymer matrix. However, the increase in the state of stress equilibrium solely by adjusting the CF is not adequate. In order to achieve elevated state of stress equilibrium, large extent of creep is necessary to increase the formation of more “quasi” crosslink networks. As a consequence, the formation of “quasi” crosslink networks between several granules may also be resulted (Illustration 4.2).

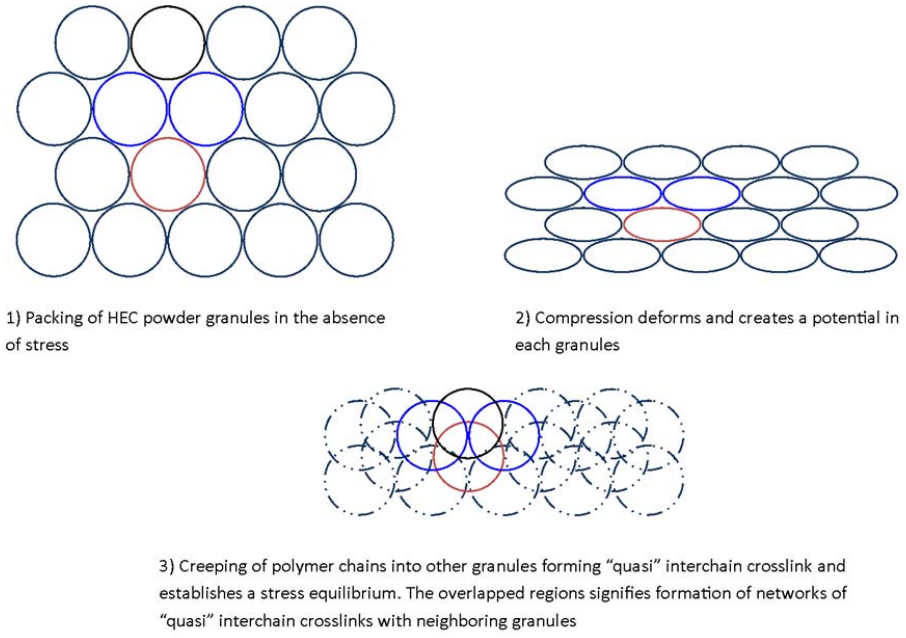

Illustration 4.2: Schematics representing the formation of crosslink networks between neighboring granules due to effect of compression

Since creep is essentially a time dependent phenomenon, the application of CF with low exertion duration will result in a less effective formation of “quasi” cross-linkages. As a consequence, the

findings (Figure 4.1) reports an initial increase followed by a plateau in the performance of the pore characteristics of the AC produced with increasing CF at a low holding time. The breakthrough, in the pore characteristics of the AC, derived from using a combination of high CF and holding time as the compression conditions, is postulated due to a larger extent of creep. The longer holding time, coupled with high CF, results in a larger concentration of "quasi" cross linkages to be formed with greater number of chains. As a result, the pellets are synthesized at a highly "stressed" state prior the HTT processes.

Supporting evidence on the effect of CF conditions on the creep phenomenon can be derived from the bulk densities of the pellets after the pre-treatment process (Table 4.1). The change in the thickness of pellets, Δx, is calculated using the thickness of the pellets synthesized under the compression conditions of 2 metric ton for 15 minutes as the reference in accordance to the respective mass loadings. For example, Δx for 5-8-60-P is calculated by the difference between the thickness of the pellet of 5-2-15-P (5.69 cm) and 5-8-60-P (5.14 cm), and Δx for 2.5-8-60-P is calculated by the difference between the thickness of the pellet of 2.5-2-15-P (2.79 cm) and 2.5-8-60-P (2.56 cm).

To develop the "quasi" crosslink networks, it is first necessary to reduce the amount of void space present between neighboring powder granules in the pellet by effect of CF. In a thick pellet, the amount of free voids due to imperfection of stacking of power granules is greater compared to a thinner pellet (Illustration 4.3). As a consequence, a thick pellet has a capacity to exhibit a higher value of Δx value compared to the thin pellets. For instance, when the CF is increased from 2 metric ton to 8 metric ton for a holding time of 60 minutes, Δx increases from 0.14 cm to 0.55 cm for the 5 g pellets. For the 2.5 g pellets, Δx increases from 0.12 cm to 0.23 cm for the 2.5 g pellets.

With a lesser amount of void spaces between neighboring granules, there is a larger inclination for chain motion. Consequently, a thinner pellet would experience a more rapid development of "quasi" crosslinks with neighboring granules. As a result, the findings show that, under the same

compression conditions, the thin pellets, in general, have bulk densities larger or equal to the thick pellets counterparts.

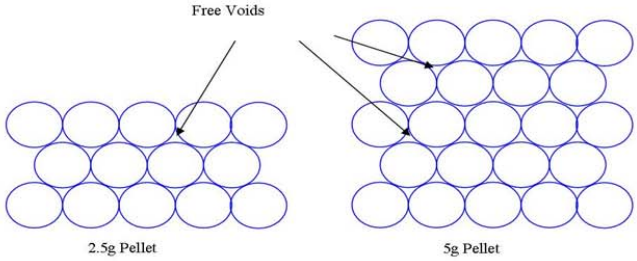

1) A larger amount of stacking of powder granules due to a higher quantity of precursors used result in more free voids present in 5g pellets.

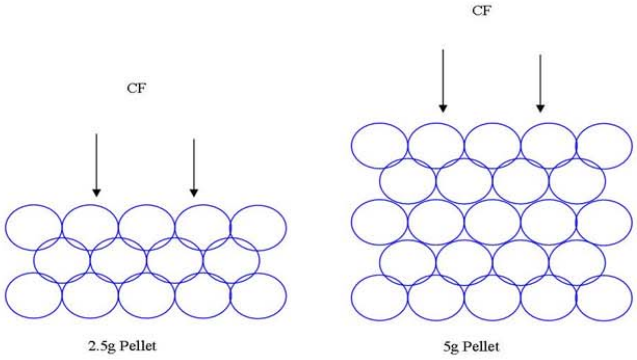

2) To develop "quasi" crosslinks with neighbouring powder granules, the reduction of free void first occur by the effect of CF. A lower amount of free void space present in 2.5g pellets promote a rapid rate of removal of free void and the formation of "quasi" crosslinks.

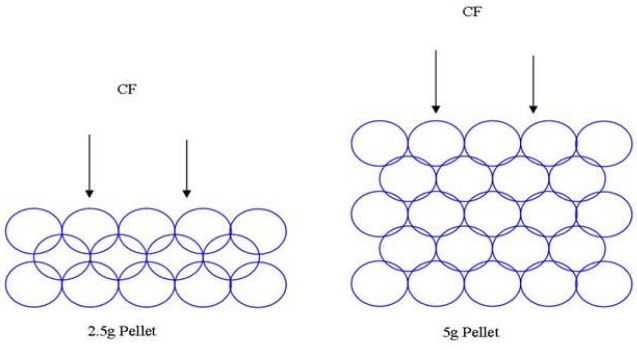

3) As a consequence, the number of interactions (represented by overlapping regions) between neighboring powder granules formed in the 2.5g pellets are greater compared to the 5g pellets.

Illustration 4.3: Schematic diagram depicting the larger extent of creep exhibited in 2.5g pellets compared with the 5 g pellets

4.3 Stress relaxation phenomenon

4.3.1 Surface generation by stress relaxation mechanism

The unique response of the HEC pellets towards compressive stress after the HTT processes can be observed at the end of the HTT processes (Figure 4.3). AC samples derived from the pre-treatment process show evidences of expansion of the carbon bodies at the end of the synthesis. Regardless of the compression conditions (CF and holding duration), AC synthesized from the thinner pellets (2.5g of HEC) depict a high extent of expansion by adopting hollow hemispherical geometries. The images of 2.5-8-15-AC are used to represent the rest of the AC samples (Figure 4.3c and Figure 4.3d). Conversely, AC produced from HEC pellets with a mass loading of 5 g have a larger resistance towards expansion and retain most of the original disc shape. However, slight curvatures are observable on the surface of the disc shape pellets. The images of HEC-5-8-15-AC are used to represent the samples (Figure 4.3a and Figure 4.3b). A greater degree of expansion can still be observed in AC samples synthesized from 5 g pellets under high CF (≥ 8 metric ton) exposed to duration of 60 minutes. For these samples, partial hollow hemisphere geometries are observed. The images of 5-10-60-AC are used to represent these samples (Figure 4.3e and Figure 4.3f). It is also noted that 2.5-2-60-AC (Figure 4.3g) is unable to maintain structural integrity.

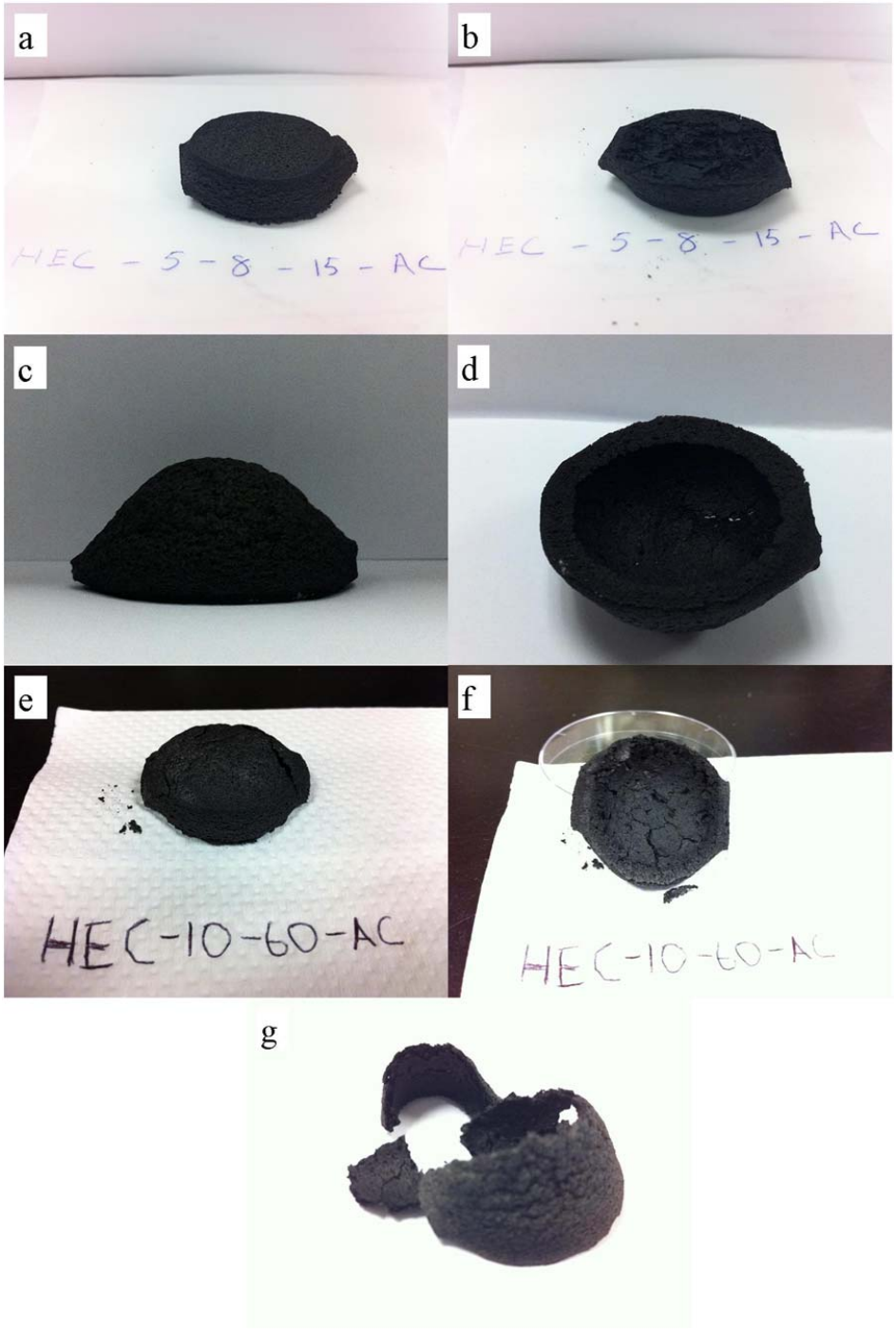

Figure 4.3: a) 5-8-15-AC (upright) b) 5-8-15-AC (inverted) c) 2. 5-8-15-AC (upright) d) 2.5-8-15-AC (inverted) e) 5-10-60-AC (upright) f) 5-10-60-AC (inverted) (g) 2.5-2-60-AC (broken).

The geometry of the AC provides several observations: firstly, a carbon body with a well defined shape is produced. Before the initiation of the HTT processes, the "quasi" crosslink networks 'freeze' the neighboring polymer chains in position and give the pellets a definite cylindrical disc shape. However, the HTT processes can damage the network by either physically untangle the "quasi" crosslink networks or by scission of the polymer chains. Since the "quasi" crosslink networks are physical in nature, they are unlikely to survive throughout the HTT processes. If the networks were to be destroyed during the HTT processes, the cylindrical disc structure will collapse. One may then expect that at the end of the process, a carbon body, devoid of any definite shape will be obtained. However, during carbonization, permanent fixations of the chains occur through aromatization. Thus, the free carbon ends, combined with other chains or ends, support the structure mechanically eventually in the synthesis process.

Secondly, tuning the parameters used in the pre-treatment process can result in an extreme geometric transformation. The surface curvature observed in the AC samples is due to effect of stress relaxation (Figure 4.3). It is typical for bodies, subjected under compressive forces, to expand against the direction of the applied load when the load is removed as a corrective mechanism to relieve compressive stress. Since stress equilibrium is achieved by the formation of "quasi" crosslink networks, the corrective response is delayed. Most of the compressive stress energy is only released through the disentanglement of the physical crosslink networks or the scission of the polymer chains during the HTT processes. During the process, one may expect that the chain motions will influence how the AC will be formed. However, the chain motions may be inhibited by the "quasi" crosslink networks and the fixation by aromatization. The inhibitions of the chain motions deter stretching and expansion of the carbon matrix. As a consequence, during the HTT processes, the thermal strain imposed on the carbon body is significant. To maintain stress equilibrium by stress relaxation and the increasing amount of thermal stress, some of the energy is converted to work done to create new surfaces. The geometric transformations of the

pellets provide physical evidence of the generation of additional surface area on a macroscopic scale. The chains expand and stretch to accommodate a new stress state and hollow hemisphere structures is adopted. The results validate that the stretching and expansion effect influences the surface area of the AC produced on a microscopic scale (Table 4.1). Further evidences are provided in the microscopic study using FESEM in Section 4.4.

The mechanical stability of the carbon bodies plays an important role in the capacity to stretch and expand. This is because premature structural failure results in an abrupt release of compressive stress energy and a less effective utilization of the stress relaxation effect. A smaller degree of stretching of the network results and may justify the poor pore characteristics of 2.5-2-60-AC (Table 4.1).

4.3.2 Role of "quasi" crosslink networks in stress relaxation phenomenon

The geometric transformation of the AC demonstrates the effectiveness of the utilization of stress relaxation to generate new surfaces from using thin pellets. A lower resistance towards stress relaxation effect is predominantly observed in thin pellets. The phenomenon is closely related to the packing of the powder granules and the development of the "quasi" crosslinks networks developed by cold compression. The lower mass content in thin pellets results in a smaller amount of granules packed in the axial direction compared to thick pellets (Illustration 4.4). Consequently, the amount of "quasi" crosslink networks developed in the axial direction by compressive forces is lower in thin pellets. The thin pellets have a lower stiffness and are more susceptible to deform during stress relaxation. A higher capacity for the chains to stretch and twist to accommodate thermal stress results in a more effective utilization of the compressive stress energy stored in thin pellets compared to thick pellets.

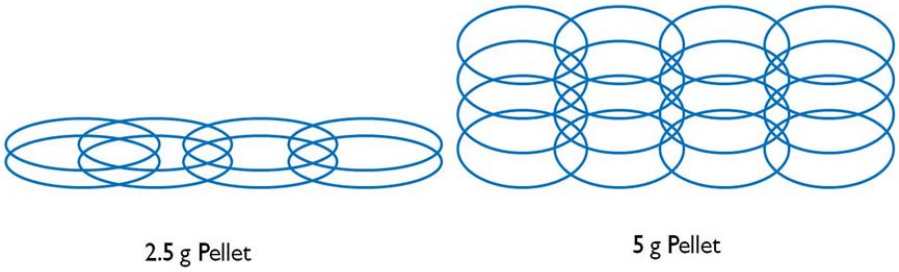

Illustration 4.4: Schematic diagram depicting the stiffness of the pellets of different thickness is dependent on the thickness of the pellet due to the quantity of "quasi" crosslink networks formed in the axial direction

The stiffness of the pellet is also dependent on the development of the "quasi" crosslink networks formed by CF. However, the sophistication of the assessment, coupled with the absence of an effective instrumentation, poses a challenge to determine the development of the "quasi" crosslink networks microscopically. However, the "quasi" crosslink networks can be resolved into 2 primary components: the axial and the radial direction. A well development of "quasi" crosslink network in the axial direction is favorable as it corresponds to the amount of stress energy associated for expansion. However, the development of "quasi" crosslink networks in the radial direction should be minimal to effectively allow a larger capacity to expand upwards in the axial direction. Hence, to have an effective stress relaxation phenomenon, it is favorable to have a prominent difference in the development of the network in the 2 directions.

Table 4.2: Postulation on the development of the networks in the HEC pellets

Pellets	Development of networks in the Axial Direction	Development of networks in the Radial Direction
5-8-15-P	Low	Low
5-8-60-P	High	Moderate
2.5-8-15-P	Moderate	Low
2.5-8-60-P	High	High

Table 4.2 postulates and compares the development of networks in the axial and radial direction for pellets 5-8-15-P, 5-8-60-P, 2.5-8-15-P and 2.5-8-60-P. The development of the "quasi" crosslink is dependent on the duration of the applied load and the thickness of the pellets. Since a thick pellet and a low duration are used for sample 5-8-15-P, it has a lower extent of development of "quasi" crosslink networks in both directions. The increase in the holding duration promotes a larger amount of chain motions and improves the development of the "quasi" crosslink networks. The development of the "quasi" crosslink networks between granules can be considered as considered "high" in the axial for 5-8-60-P. However, "moderate" level of "quasi" crosslink networks is considered to develop in the radial direction for 5-8-60-P due to the lower rate of creep compared to the thin pellets.

Rapid chain motions attributed to a low mass loading promotes formation of well-developed networks between granules. The development of the networks in the axial direction is considered to be "moderate" in 2.5-8-15-P and "low" in the radial direction. The increase in the holding duration to 60 minutes further promotes chain motions and highly developed networks are present in the axial and the radial direction in 2.5-8-60-P.

The postulation in Table 4.2 provides further evidence for the observation. A lower development of the "quasi" crosslink networks result in a lower amount of compressive stress energy developed in granules within 5-8-15-P. The effect of stress relaxation is localized and the stretching and pulling of the chain layers is not prominent compared with other samples. The increase in the holding duration improves the development of the networks in both axial and radial direction. The redistributions of the strain energy in the networks are more efficient during stress relaxation in 5-8-60-P. As a result, a greater stretching effect can be achieved and improves the turbostraticity of the carbon body.

The rapid development of the crosslink networks in 2.5-8-15-P allow a similar situation to occur in 5-8-60-P. However, the extension of the holding duration in the 2.5 g pellets also rapidly improves

the development of the networks in the radial direction. This increases the resistance towards stretching and pulling of the network and the carbon layers in the axial direction. Thus, a lower degree of stretching occurs from 2.5-8-60-P compared with 2.5-8-15-P. As a result, a disparity in the effect of extending the holding duration at elevated load is reported.

4.4 FESEM characterization

4.4.1 Effect of HTT on powdered HEC granules

Without the effect of cold compression, the carbonization of the HEC polymer results in the formation of continuous carbon film (Figure 4.4a). Prior carbonization, the powder granules are loosely packed and stacked on top of one another (Illustration 4.2). During carbonization, the intra-chain "quasi" crosslink networks collapse. The weakened mechanical stability within each granule causes loss of 3 dimensional characteristics. Neighboring granules coalesce to reduce the total surface energy and results in the formation of a continuous flat film with a lack of surface traits. The activation process by CO_2 is thus limited to the active sites on the surface of the continuous film, resulting in the formation of a refined surface (Figure 4.4b). The poor surface morphologies of the AC results in the unimpressive pore characteristics reported by N_2 adsorption (Table 4.1).

4.4.2 Microscopic study on surface generation by stress relaxation phenomenon

The carbon bodies (carbonaceous material and the AC) derived from HEC pellets using cold compression pre-treatment yield a wide range of surface information. The surface characteristics, such as presence of crevices and ridges on the surface, provide evidences of surface generation due to stress relaxation. In particular, these surfaces information on the carbon bodies are highly noticeable when high CF (≥8 metric ton) is used to synthesize the HEC pellets. Thus, microscopic studies of these carbon bodies are used to assess the effect of stress relaxation phenomenon on surface generation on AC (Figure 4.4).

The application of CF envelops neighboring granules together by favoring polymer chains to creep and form "quasi" crosslink networks. The networks strengthen the mechanical stability of the entire body and prevent the granules to coalesce during carbonization. A carbon body comprised of a granular surface such as 5-8-15-C (Figure 4.4c) may be obtained. A greater extent of creep promotes a larger extent for polymer chains to creep into neighboring granules. The granules start

to lose their spherical characteristics and become more blended into neighboring granules. A slightly more continuous carbon surface such as 2.5-8-15-C (Figure 4.4g) may be obtained. Further increase in the creep effect causes the granules to be well blended into each other and a continuous surface such as 5-8-60-C (Figure 4.4e) and 2.5-8-60-C (Figure 4.4i) is observed.

Inherently, the preliminary networks developed affect the type of surface information which will be developed in the carbon bodies. For instance, a low extent of creep is postulated for 5-8-15-P associate with a mediocre mechanical stability. Thus, the capacity for polymer chains to stretch and expand is weaker. As a result, during stress relaxation, a lesser extent of stretching and pulling is resulted and the network fractures and formation of crevices occurs. Hence, the compressive stress energy is not effectively utilized in this sample and thus, a lower amount of stretching and twisting to form surface morphologies. After the activation processes, the crevices become more prominent. Hence, this results in mediocre pore characteristics of S_{BET} of 1370 m^2/g and pore volume of 0.86 cc/g.

The effect of stress relaxation can be further exemplified by the carbon body 2.5-8-15-C. Due to the same compression conditions (8 metric ton for 15 minutes) 2.5-8-15-C has a similar granular surface. However, the higher capacity to deform and accommodate thermal strain results in the formation of ridges. The activation process further develops the ridges into new surfaces (Figure 4.4h). Hence, this results in very high pore characteristics of S_{BET} of 2080 m^2/g and pore volume of 1.43 cc/g. This phenomenon is also observed in both 5-8-60-C and 2.5-8-60-C. However, as the networks are better developed, the stronger resistance against stress relaxation causes the formation of larger surface characteristics as observed in Figure 4.4.

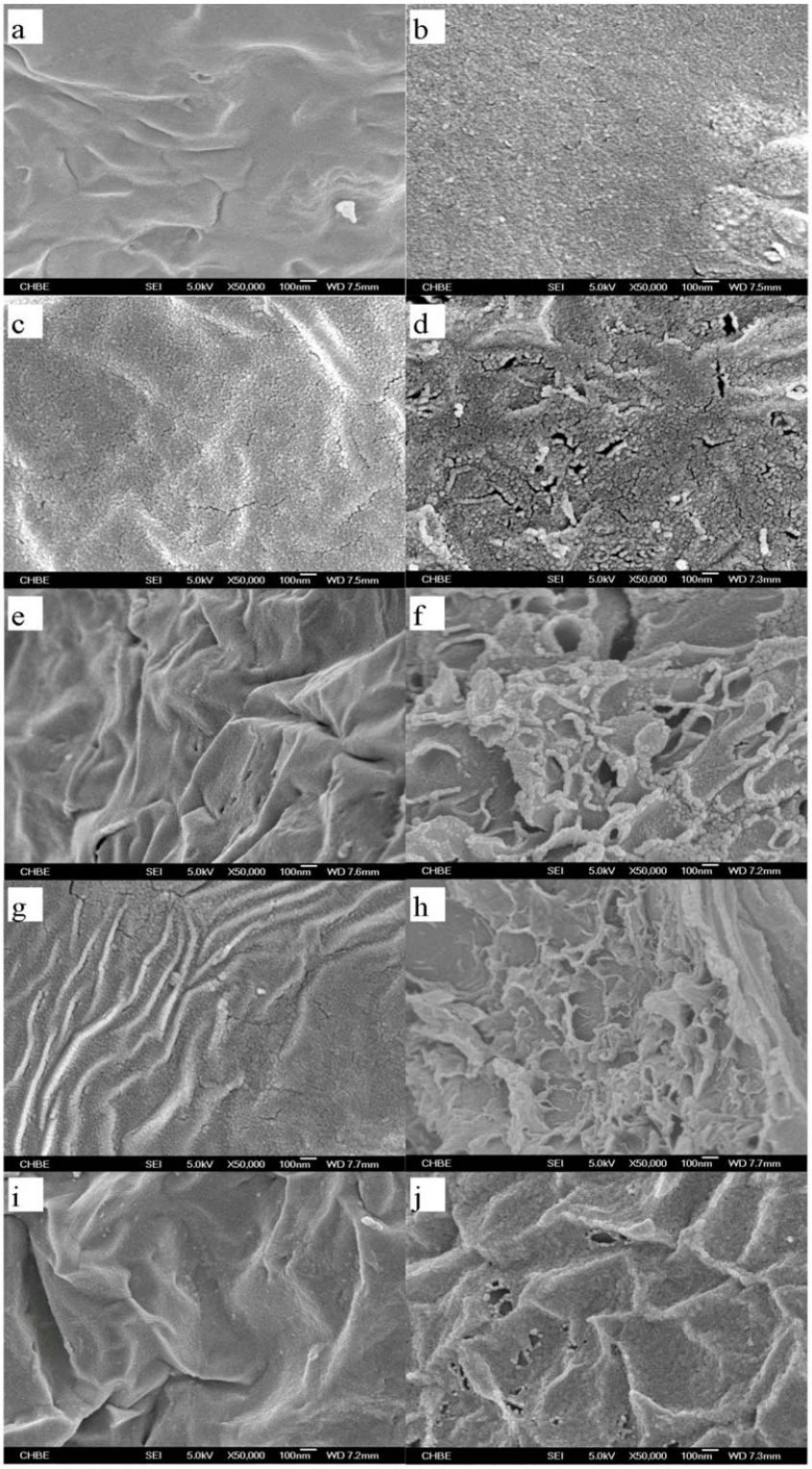

Figure 4.4: FESEM images of the carbonaceous materials and the respective AC a) 5-0-0-C b) 5-0-0-AC c) 5-8-15-C d) 5-8-15-AC e) 5-8-60-C f) 5-8-60-AC g) 2.5-8-15-C h) 2.5-8-15-AC i) 2.5-8-60-C j) 2.5-8-60-AC

4.5 Determining Functionalities present in carbonaceous materials

4.5.1 ^{13}C nuclear magnetic resonance and FTIR

The ^{13}C NMR is used to determine which moieties are predominant during the carbonization process. The ^{13}C NMR spectra of 5-0-0-C, 5-8-60-C and 2.5-8-15-C (Figure 4.5) reveal that the aromatic functional groups (125 ppm) are dominant in all the carbonaceous materials at the end of the carbonization process. Aliphatic groups (0-45 ppm) and ketones and aldehydes functionalities (190-210 ppm) are present in both 5-0-0-C and 2.5-8-15-C. Carboxylic and esters (165-190 ppm) and aliphatic ether (50-90 ppm) moieties are absent in all the carbonaceous materials [23, 24]. 2.5-8-15-C and 5-8-60-C are chosen to compare with 5-0-0-C because the surface area and the pore volumes of the AC produced are the highest for the respective mass loading used to synthesize the polymer pellets.

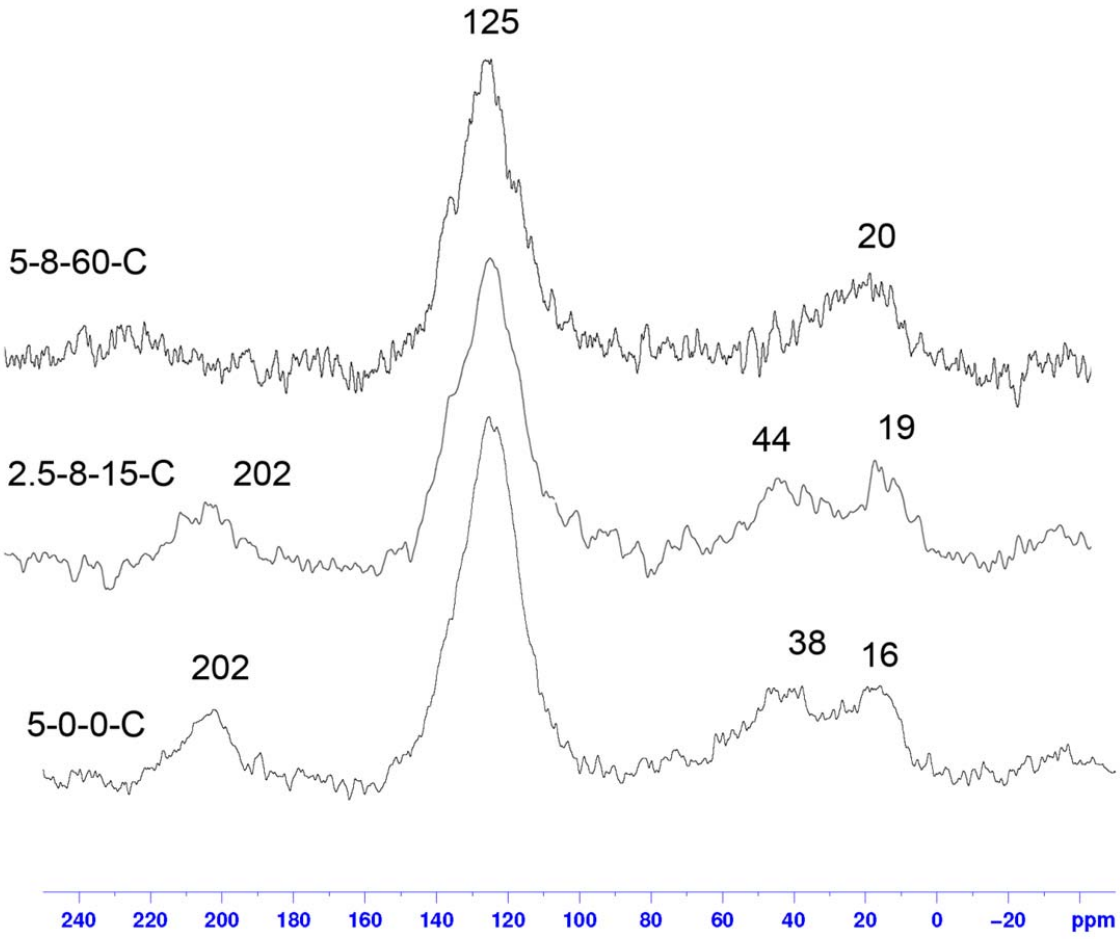

Figure 4.5: Solid state ^{13}C NMR of the carbonaceous material of 5-0-0-C, 2.5-8-15-C and 5-8-60-C

Since the C=C functionality is chemically stable, the formation of large abundance of the aromatic functional groups is expected. It is also evident that moieties that are less chemically stable or thermodynamically less feasible to develop are unlikely to be present after carbonization. Based on the chemical structure in Figure 4.6, the carbons in the main chain have an oxygen atom bonded in alternation. Thus, it is unlikely for carboxylic acid and esters functionalities to form. This is because an oxygen atom has to be created by scission from neighboring site and migrate specifically for bond formation. In addition, the formation of COO moieties has to occur as a hanging chain near the edges of the carbon planes to establish chemical stability. The process is

less thermodynamically favored since formation of the COO moieties promotes steric hindrance and increases the stress state experienced in the networks.

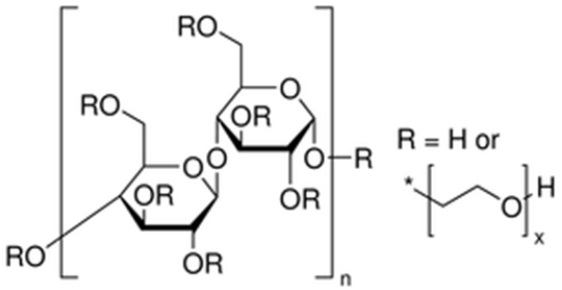

Figure 4.6: Chemical structure of HEC

Since carbonization essentially involves the removal of heteroatoms, the amount of C-O moieties is expected to be low or absent. Although the C-O moieties are not detected by ^{13}C NMR, the presence of the C-O moieties in the carbonaceous materials after carbonization should not be ruled out. The low occurrence of the ^{13}C atoms and the inability to detect the presence of C-O moieties associated with the ^{12}C atoms open up the possibilities of the presence of the C-O moieties in the carbonaceous materials.

The C=O moieties are absent in the initial HEC polymer structure and are thus generated during carbonization. Thermodynamically, the formation of the C=O moieties is favored compared to the C-O moieties. This is because the presence of the π bonds in the C=O moieties have a higher chemical stability compared to the C-O moieties. In addition, the π bonds also favor the formation of resonance structures during carbonization. The ease of generating C=O moieties through cleaving off one of the C-O bonds present in the C-O-C structure followed by a stabilization of the structure by resonance effect suggest that the C=O moieties play an important role in the carbonization chemistry of HEC.

FTIR spectra of the carbonaceous materials show that there is minimal variation in the chemical compositions after carbonization (Figure 4.7). However, the results also confirmed that also

confirmed in all the carbonaceous samples, the C=O moieties (1694 cm^{-1}) [15], aromatic ring structures (1560 cm^{-1}) and C-O moieties (1204 cm^{-1}, 1367 cm^{-1}, 1433 cm^{-1}) are present. It may be worthwhile to note that carbonaceous materials derived from the pre-treatment show weak hydroxyl stretching (~3421 cm^{-1}). The spectra suggest that cold compression creates a prominent structural change in the carbonaceous material on the side – chain functionalities during carbonization. In addition, this observation provides further evidence of the significance of the side chain group on the effect of compression.

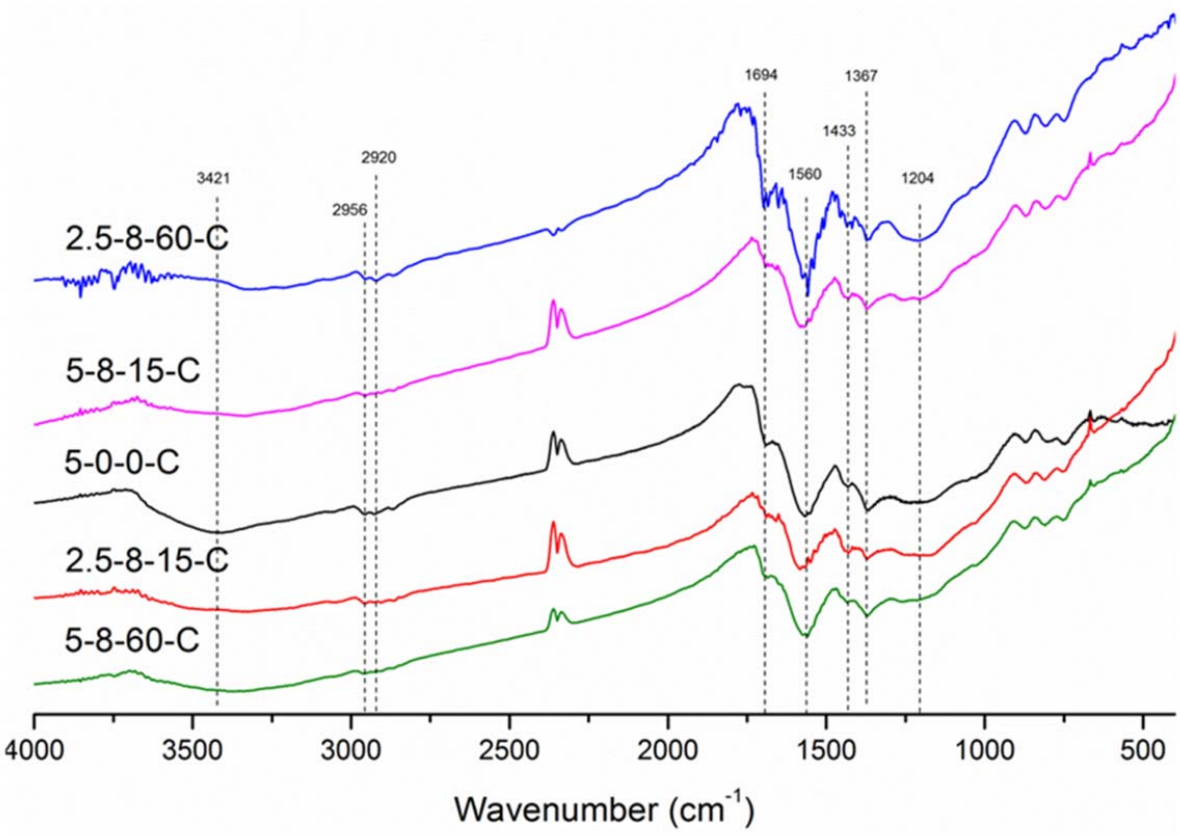

Figure 4.7: FTIR spectra of carbonaceous materials of 5-0-0-C, 5-8-15-C, 5-8-60-C, 2.5-8-15-C and 2.5-8-60-C

4.5.2 X-ray photoelectron spectroscopy

Table 4.3: Binding energy associated with the functionalities present in the carbonaceous samples

Functionalities	Binding Energy (eV)	Uncertainty (± eV)
C-C/ C=C	284.6	0.1
C-O	285.7	0.1
C=O	287.3	0.2
COO	289.0	0.2
Plasmon	290.8	0.2

The C 1s spectra of the carbonaceous materials obtained from various pellet samples exhibit similar peak characteristics with the C 1s spectrum obtained from the powder form. In all spectra, the C 1s peak is deconvoncated into 5 peaks, representing the C-C/C=C, C-O, C=O, COO and the plasmon peaks [15, 21] (Table 4.3). Among all the other samples, the C 1s spectra of the samples 2.5-8-15-C and 2.5-2-60-C show distinctive disparities compared with other carbonaceous samples (Figure 4.8). The spectrum of 5-0-0-C is used to represent the rest of the spectra that shares similar spectrum. The spectrum of 2.5-8-15-C exhibits a very broad C 1s peak and 2 distinct peaks can be deconvulated from the spectrum of 2.5-2-60-C. The spectra of the remaining samples bore high resemblance with the spectrum of 5-0-0-C.

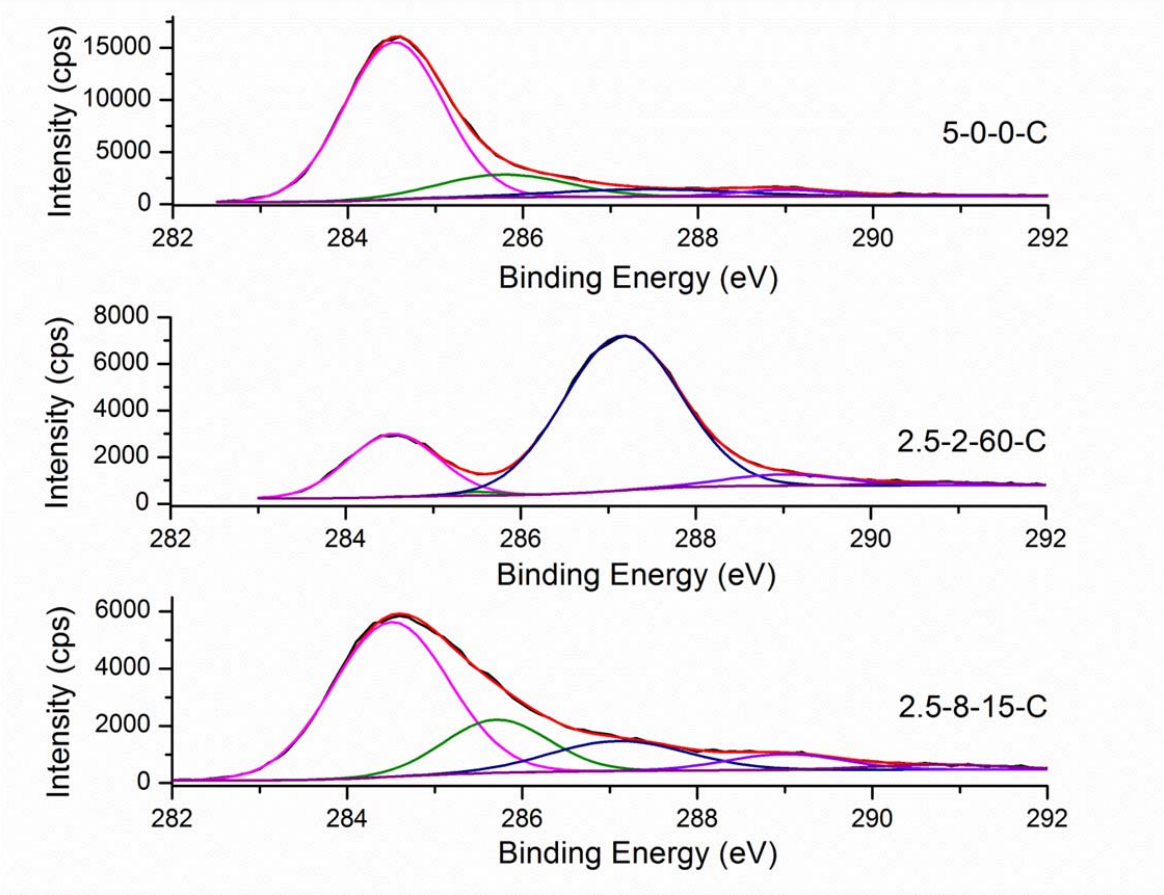

Figure 4.8: XPS spectra of carbonaceous samples of 5-0-0-C, 2.5-2-60-C and 2.5-8-15-C

Table 4.4: Moieties compositions present in carbonaceous sample determined by deconvoncation of C 1s peak from respective XPS spectra

		Mass loading 2.5g	Mass loading 5g
Samples	Peaks	Relative %	
2-15-C	C-C/ C=C	63.8	53.4
	C-O	24.4	34.0
	C=O	6.6	6.3
	COO	4.7	5.1
	Plasmon	0.5	1.2
2-60-C	C-C/ C=C	22.2	67.3
	C-O	0.7	13.5
	C=O	70.7	14.3
	COO	5.1	2.7
	Plasmon	1.3	2.2
8-15-C	C-C/ C=C	59.7	64.8
	C-O	18.5	25.3
	C=O	13.6	3.5
	COO	6.1	5.0
	Plasmon	2.1	1.4
8-60-C	C-C/ C=C	62.2	63.3
	C-O	28.8	21.8
	C=O	3.5	10.3
	COO	4.0	3.6
	Plasmon	1.5	1.0
5-0-0-C	C-C/ C=C	75.3	
	C-O	14.0	
	C=O	6.5	
	COO	3.1	
	Plasmon	1.0	

The compositions of the functional groups present in the carbonaceous samples are tabulated in Table 4.4. Previous discussion on the improbability of the formation of the carboxylic functionalities in Section 4.5.1, together with the comparable contents among the samples obtained from XPS peak fitting (Table 4.4). Since carboxylic functionalities present in the carbonaceous materials are not observable in ^{13}C NMR and the contents are comparable in XPS for the generated samples, the contributions by the carboxylic functionalities in the carbonization process are not essential. Results from ^{13}C and FTIR spectra provide strong indication that the C=C, C=O and the C-O moieties are active participants in the carbonization process. Thus, the XPS analysis would

also place strong emphasis on the surface oxygenated complexes involving C-O and C=O and the graphitic carbons (C-C/ C=C moieties).

4.5.3 Significance of the C-O moieties in the carbonaceous materials

The C-O content present in the carbonaceous species from the powder form is among the lowest (excluding 2.5-2-60-C). In the absence of external forces, the polymeric chains are free to reform in response to intra-chain stress arising during carbonization. The intra-chain "quasi" crosslink networks readily collapse to relieve the intra-chain stress and facilitate the formation of a more stable carbon structure associated with high graphitic carbon. Conversely, high content of C-O moieties are detected in carbonaceous materials synthesized by cold compression. A higher resistance towards formation of graphitic carbon is exhibited by the carbonaceous samples generated from cold compression. Since both 2.5-2-15-C and 5-2-15-C can represent the lowest degree of "quasi" crosslink networks present amongst the samples, they should exhibit characteristics that are highly identical to the form of the powder. However, compared with 5-0-0-C (14.1%), both 2.5-2-15-C and 5-2-15-C have a higher C-O content present (24.4% and 34.0% respectively).

It is postulated that the C-O moieties improves the mechanical stability of the carbon matrices. The single bond in the C-O moieties are more adaptable to bond stretching and rotations compared to sp^2 hybridized aromatic carbon or the C=O functionalities. Although aromatization and the formation of C=O functionalities increases the chemical stability of the carbon matrices, the rigidness of the π bonds create conformation restrictions. Stretching of the planar structures associated with the development of sp^2 hybridized bonds create strain on the carbon matrix. The flexibility of C-O moieties can serve as stress-strain regulators and allow a larger extent of stretching and pulling of the carbon layers. Thus, a larger amount of C-O moieties are present in carbonaceous materials synthesized with the cold compression pre-treatment.

The XPS peak fit (Table 4.4) reveals 2.5-2-60-C has a low graphitic carbon content (22.2%), an extremely low content of C-O (0.7%) and a very high content of C=O (70.7%) moieties provide further evidence. The high C=O moieties and low graphitic carbon content depict that after carbonization, small polyaromatic planes are formed in 2.5-2-60-C. In addition, the low content of the C-O moieties stress-strain regulators also suggest that after carbonization, the carbon matrix has a low tolerance for stress-strain variation. The mechanical stability developed after carbonization of 2.5-2-60-C is weak and activation at high temperature disintegrates the aromatic planes further and the structure eventually collapses (Figure 4.3g).

4.5.4 Influence of cold compression on formation of surface oxygen

The influence of each parameter (CF, mass loading and the holding duration) on the formation of the surface oxygen functionalities is haphazard. However, the chemical change in the carbonaceous materials due to cold compression prior carbonization can be broken into 3 categories: (1) A very high C=O moieties and very low C-O moieties are present (e.g. 2.5-2-60-C), (2) a high C-O content (20-30%) and a low C=O (3-6%) content (e.g. 5-0-0-C) and (3) a comparable ratio of the C=O and the C-O moieties are present (e.g. 2.5-8-15-C).

The comparable ratio of C-O and C=O present in carbonaceous samples of 5-2-60-C, 2.5-8-15-C and 5-8-60-C suggest a possibility of an established equilibrium between the 2 moieties due to effects of cold compression. A likely mechanism that potentially creates the differences in the ratio of the surface oxygen is the “keto-enol” tautomerism. Although the “keto” form is highly preferred due to the chemical stability, the equilibrium can be shifted towards the formation of “enol” by aromaticity and conjugations during the carbonization process. This may also further explain although C=O moieties are chemically more stable compared to the C-O moieties, a larger content of C-O and a low content of C=O moieties are present in most samples after carbonization.

Another possibility for the variation in the content of the surface oxygen present is the effect of stretching due to stress relaxation. Under CF of 8 metric ton, when the duration increases from 15

to 60 minutes, the C-O content increases and the C=O content decreases for carbonaceous materials synthesized from 2.5 g pellets. For the carbonaceous materials synthesized from HEC pellets with a mass loading of 5 g, the C-O content decreases while the C=O content increases. Since scission of the C-O bonds effectively relieves the strain experienced in the matrices, a lower content of C-O moieties is observed in 2.5-8-15-C and 5-8-60-C. The larger effect of stretching prevents immediate reaction of the free active ends due to the increased microscopic distance, giving a higher potential for the formation of C=O moieties.

4.6 Pore characteristics of AC

4.6.1 Adsorption Isotherm

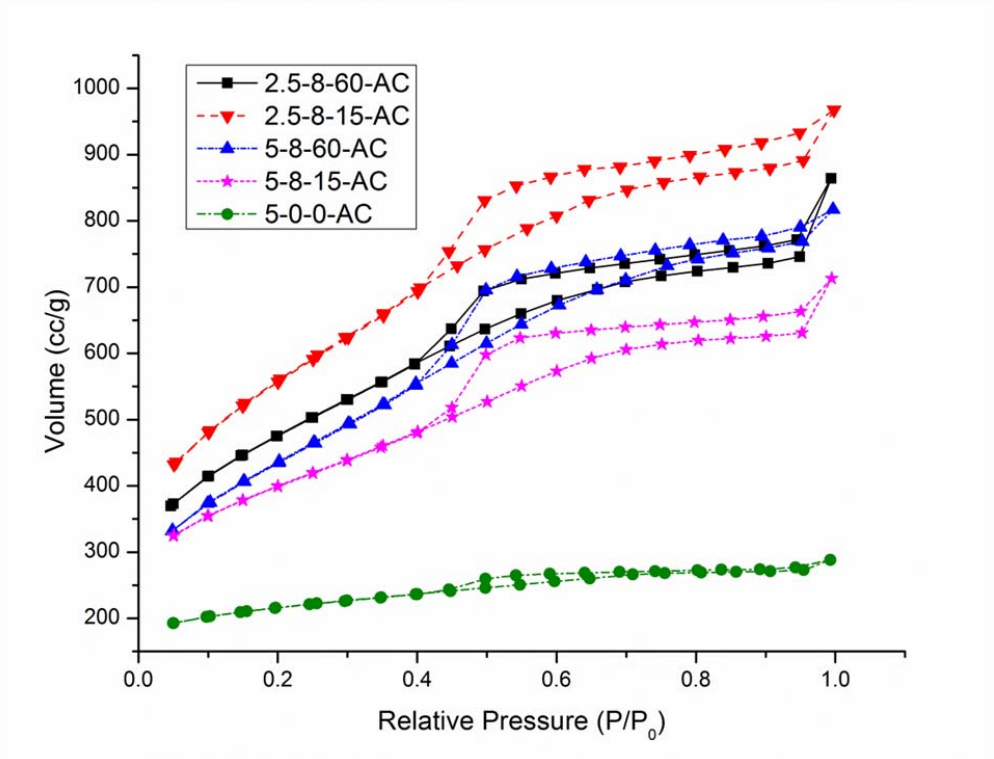

Figure 4.9: Adsorption Isotherm of 5-0-0-AC, 5-8-15-AC, 5-8-60-AC, 2.5-8-15-AC and 2.5-8-60-AC

All the AC produced by the HEC polymer regardless of pre-treatment have Type IV adsorption isotherm characteristics (Figure 4.9). This suggests that the adsorption can takes place on open surface but also in mesopores. The AC produced from HEC has good adsorption characteristics.

4.6.2 Pore characterization

Table 4.5: Pores characterization of AC synthesized from effects of high CF

Sample	S_{BET} (m^2/g)	V_{Total} (cc/g)	V_{Micro} (cc/g)	V_{Meso} (cc/g)	$\frac{V_{Meso}}{V_{Total}}$
5-0-0-AC	810	0.35	0.24	0.11	0.32
5-8-15-AC	1370	0.86	0.51	0.35	0.41
5-8-60-AC	1710	1.07	0.60	0.47	0.44
2.5-8-15-AC	2075	1.43	1.08	0.35	0.24
2.5-8-60-AC	1790	1.30	0.46	0.84	0.65

AC produced using HEC as the precursors are micropores dominant (Table 4.5). Cold compression prior carbonization favors the formation of both micro and mesopores formed. Formation of mesopores can be enhanced by increasing the holding duration at elevated load on the polymer pellets prior carbonization. The improved pore textures can be accounted by the larger degree of turbostracity demonstrated in the FESEM images (Figure 4.4).

All the AC produced has characteristic pore widths of approximate diameter of 18.0 Å, 27.4 Å and 36.3Å (Figure 4.10). The observations reflect that the effect cold compression prior carbonization has negligible effect on overall microscopic carbon skeleton structure.

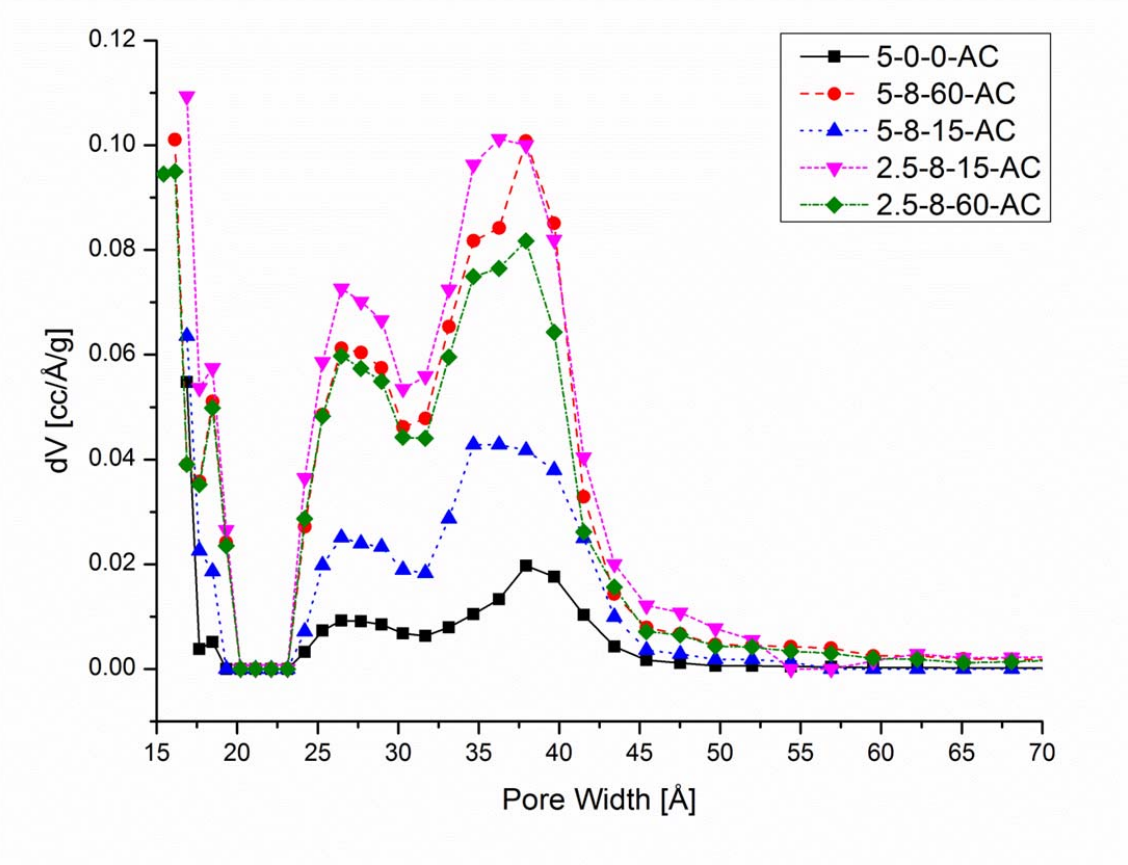

Figure 4.10: Pore Size Distribution of AC synthesized from HEC pellets subjected to high stress prior carbonization

4.7 H_2S adsorption capability

Table 4.6: H_2S adsorption assessment of AC synthesized from effects of CF

Sample	S_{BET} (m^2/g)	Pore Volume (cc/g)	Bed Length (mm)	Breakthrough Time (min)	Breakthrough Capacity (mg/g)	pH
5-0-0-AC	810	0.35	8.0	61.86	13.0	10.3
5-8-15-AC	1370	0.83	8.5	71.09	13.7	10.0
5-8-60-AC	1620	1.17	8.0	84.55	16.1	9.7
2.5-8-15-AC	2080	1.43	7.5	74.44	14.3	8.8
2.5-8-60-AC	1790	1.30	8.0	112.00	21.6	9.6

The rank in terms of the performance of the breakthrough capacity is in the order of 5-0-0-AC < 5-8-15-AC < 2.5-8-15-AC < 5-8-60-AC < 2.5-8-60-AC (Table 4.6). The extension of the holding duration of the CF from 15 minutes to 60 minutes produces the most desired performance for adsorption of H_2S. A negative correlation between the surface basicity and the surface area of the AC is established.

It is known that the surface basicity and the pore characteristic of the AC affect the adsorption capacity of acidic gas such as H_2S. It may then be debatable to consider which factor is more effective in enhancing the adsorption capability of H_2S. A comparison made between 5-8-15-AC with 2.5-8-15-AC show that an increase in the surface area of the AC (710 m^2/g) corresponds to a higher adsorption performance of H_2S (an increase of breakthrough capacity of 0.6 mg/g). One may, however, attribute the sluggish adsorption to a significant drop in the surface basicity (a decrease in pH of 1.2). A comparison between 2.5-8-15-AC with 2.5-8-60-AC reflects that the lower extent of reduction of the surface area of AC (290 m^2/g) results in a prominent effect on the adsorption performance for H_2S is observed (an increase in breakthrough capacity of 7.3mg/g).

One may then also contribute to the improved adsorption performance to the higher basicity of the AC in 2.5-8-60-AC. However, ambiguity occurs when 5-8-60-AC is compared with 2.5-8-60-AC. Although both samples have the similar surface basicity (pH of 9.6-9.7), an increase in the S_{BET} ($170 m^2/g$) have a significant improvement in the adsorption capacity (an increase of 5.5 mg/g). The discrepancy in the results suggests that, other than the surface area and the basicity of the AC, there may be other factors that have a strong impact on the performance. A comparison made from Table 4.5 and Table 4.6 show a prominent positive correlation between the mesopore volume and the breakthrough capacity. It is postulated that a larger mesopore volume facilitates and give access to more available adsorption sites. Although AC characterized by N_2 adsorption has a higher surface area, at ambient conditions (25ºC), the adsorption kinetics is likely to be slow. At the given experiment conditions, the mass transfer of the H_2S gas in the carbon matrix is slower than the adsorption rate. As a consequence, the adsorbent may not be fully utilized. The significance of the mesopores can further be validated by the 2.5-8-15-AC. This sample possesses a high degree of micropores and a low mesopores volume. It is postulated that the low mesopores present in 2.5-8-15-AC reduces the accessibility to adsorption sites and thereby reducing the adsorption efficiency compared with other samples. In addition, a cross-over in the breakthrough capacity graph (Figure 4.11) is detected between sample 2.5-8-15-AC and 5-8-60-AC further reinforces the postulation.

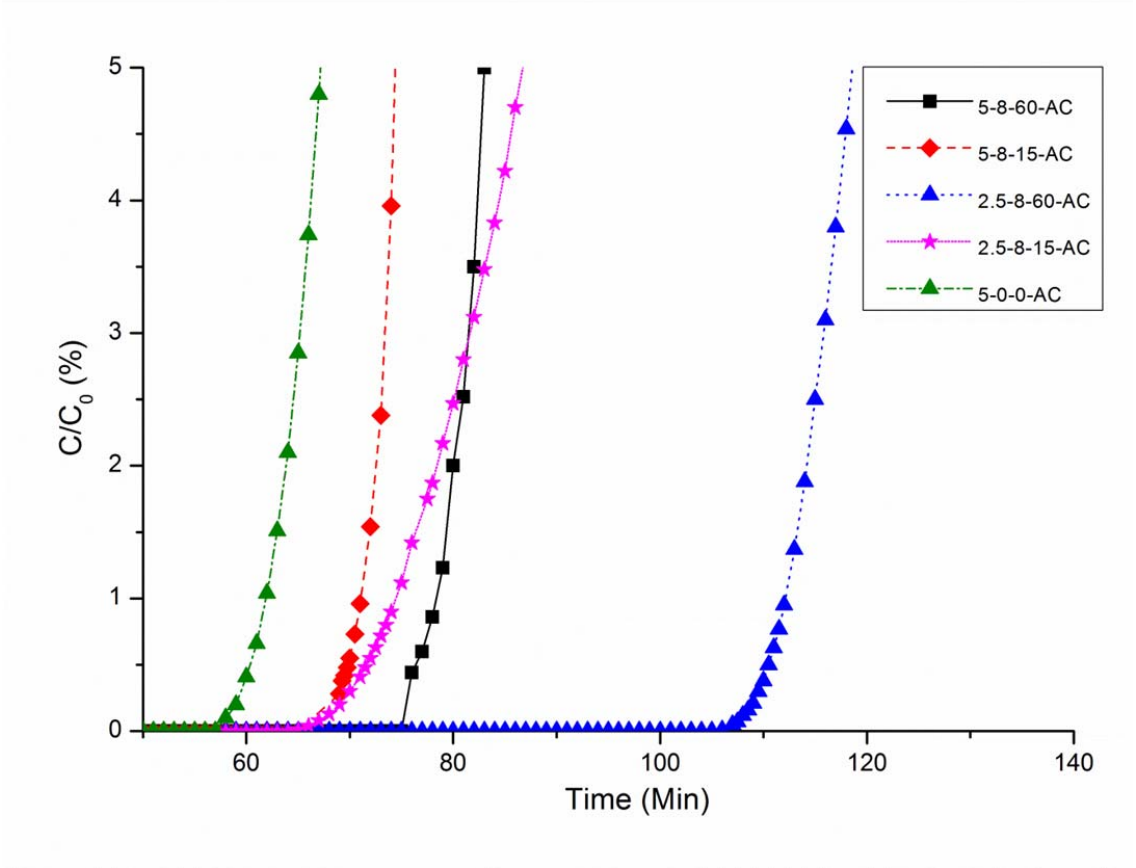

Figure 4.11: Section of the breakthrough curves of respective AC investigated for the H_2S adsorption performance

5 Conclusion

Porous AC can be synthesized from HEC pellets and are tunable by the compression conditions used to synthesize the pellets. The compression conditions and the mass loading influence the degree of creep exhibited by polymer chains. The different extent of "quasi" crosslinks networks developed due to creep creates a variation of stress in the axial and the radial direction. The variation in the stress developed creates a variation in the forces within polymer/carbon matrix by stress relaxation during carbonization. FESEM images demonstrate a prominent change in morphologies due to the combination of the effects of cross-links and stress relaxation. Functionality characterization by ^{13}C NMR, FTIR and XPS suggest that the pre-treatment process affects the formation of surface oxygen moieties. H_2S adsorption reflects that although the surface basicity and the surface area of the AC are critical to the adsorption performance for H_2S, the amount of mesopores present play a more critical factor. The practicability of developing porous carbons for adsorption of H_2S is also established.

6 Potential Development

The establishment of this work open up several other potential developments:

- Investigation of suitability of other precursors

Since the structural response is dependent on the intrinsic properties of the material, it is probable that the process to produce highly porous AC may not be suitable for all polymeric materials. At this point of the investigation work, it is postulated that the linear pendant side chain is essential in developing the "quasi" crosslink networks. The FTIR spectra reveal that the OH stretching is affected by the effect of the pre-treatment. Thus, this phenomenon suggests that the process could be largely dependent on the side chain groups of the polymer used. A detailed establishment of the essential traits of the pendant side chain groups on the formation of porous AC through the implementation of this synthesis process may prove to be beneficial.

- Incorporation of additional functionalities

Should an effective generalization on the types of precursors that are suitable for the pre-treatment process, investigation work by incorporating additional functionalities may be implemented. Polymeric materials with other functionalities (nitrogen, sulphur, etc) that have similar chemical structure as HEC may be used as the precursor. AC produced from these polymeric materials with additional functionalities may provide enhanced performance.

- Usage in other frontiers

Since carbon materials are widely used in different frontiers, the practical usage, especially in high value-small volume applications, is yet to be explored.

7 References

1. Guo, Z., Zhu, G., Gao, B., Zhang, D., Tian, G., Chen, Y., Zhang, W and Qiu, S, *Adsorption of vitamin B12 on ordered mesoporous carbons coated with PMMA.* Carbon, 2005. **43**(11): p. 2344-2351.
2. Shen, W., Wang, H., G, R and Li, Z, *Surface modification of AC fiber and its adsorption for vitamin B1 and folic acid.* Colloids and Surfaces A: Physicochemical and Engineering Aspects, 2008. **331**(3): p. 263-267.
3. Fuertes, A.B, Lota, G., Centeno, T.A and Frackowiak, E, *Templated mesoporous carbons for supercapacitor application.* Electrochimica Acta, 2005. **50**(14): p. 2799-2805.
4. Guan, C., Loo, S., Wang, K and Yang, C, *Methane storage in carbon pellets prepared via a binderless method.* Energy Conversion and Management, 2011. **52**(2): p. 1258-1262.
5. Zhang, T., W.P. Walawender, and L.T. Fan, *Grain-based AC for natural gas storage.* Bioresour Technol, 2010. **101**(6): p. 1983-91.
6. Inomata, K., Kanazawa, K., Urabe, Y., Hosono, H and Araki, T, *Natural gas storage in AC pellets without a binder.* Carbon, 2002. **40**(1): p. 87-93.
7. Marsh, H. and F. Rodríguez-Reinoso, *Chapter 5 - Activation Processes (Thermal or Physical)*, in *AC*2006, Elsevier Science Ltd: Oxford. p. 243-321.
8. Kandasamy, R., Kennedy, L., Vidya, C., Boopathy, R and Sekaran, G, *Immobilization of acidic lipase derived from Pseudomonas gessardii onto mesoporous AC for the hydrolysis of olive oil.* Journal of Molecular Catalysis B: Enzymatic, 2010. **62**(1): p. 58-65.
9. Li, L., S. Liu, and J. Liu, *Surface modification of coconut shell based AC for the improvement of hydrophobic VOC removal.* J Hazard Mater, 2011. **192**(2): p. 683-90.
10. Petit, C., K. Kante, and T.J. Bandosz, *The role of sulfur-containing groups in ammonia retention on AC.* Carbon, 2010. **48**(3): p. 654-667.

11. Yates, M., Blanco, J., Avila, P and Martin, M.P, *Honeycomb monoliths of AC for effluent gas purification.* Microporous and Mesoporous Materials, 2000. **37**(1–2): p. 201-208.

12. Yue, Z. and J. Economy, *Synthesis of highly mesoporous carbon pellets from carbon black and polymer binder by chemical activation.* Microporous and Mesoporous Materials, 2006. **96**(1-3): p. 314-320.

13. Alcañiz-Monge, J., Trautwein, G., Pérez-Cadenas, M and Román-Martínez, M.C, *Effects of compression on the textural properties of porous solids.* Microporous and Mesoporous Materials, 2009. **126**(3): p. 291-301.

14. Brown, R.P. and F.N.B. Bennett, *Compression stress relaxation.* Polymer Testing, 1981. **2**(2): p. 125-133.

15. Sun, M. and L. Hong, *Impacts of the pendant functional groups of cellulose precursor on the generation of pore structures of AC.* Carbon, 2011. **49**(7): p. 2173-2180.

16. Marsh, H. and F. Rodríguez-Reinoso, *Chapter 4 - Characterization of AC*, in *AC*2006, Elsevier Science Ltd: Oxford. p. 143-242.

17. Marsh, H. and F. Rodríguez-Reinoso, *Chapter 6 - Activation Processes (Chemical)*, in *AC*2006, Elsevier Science Ltd: Oxford. p. 322-365.

18. Shafeeyan, M.S., Daud, W., Houshmand, A and Arami-Niya, A, *Ammonia modification of AC to enhance carbon dioxide adsorption: Effect of pre-oxidation.* Applied Surface Science, 2011. **257**(9): p. 3936-3942.

19. Seredych, M. and T.J. Bandosz, *Adsorption of hydrogen sulfide on graphite derived materials modified by incorporation of nitrogen.* Materials Chemistry and Physics, 2009. **113**(2-3): p. 946-952.

20. Montgomery T. Shaw and W.J.M., *Introduction To Polymer Viscoelasticity.* 2005: p. 199.

21. Sevilla, M. and A.B. Fuertes, *The production of carbon materials by hydrothermal carbonization of cellulose.* Carbon, 2009. **47**(9): p. 2281-2289.

22. Cui, H., S.Q. Turn, and M.A. Reese, *Removal of sulfur compounds from utility pipelined synthetic natural gas using modified AC.* Catalysis Today, 2009. **139**(4): p. 274-279.

23. Cheng, H.N., Wartelle, H., Klasson, K.T and Edwards, J.C, *Solid-state NMR and ESR studies of AC produced from pecan shells.* Carbon, 2010. **48**(9): p. 2455-2469.

24. Kalaitzidis, S., Georgakopoulos, A., Christanis, K and Lordanidis, A, *Early coalification features as approached by solid state 13C CP/MAS NMR spectroscopy.* Geochimica et Cosmochimica Acta, 2006. **70**(4): p. 947-959.